Title: MAPK/ERK Activation in Macrophages Promotes *Leishmania* Internalization and Pathogenesis

Running title: ERK1/2 facilitates *Leishmania* internalization

Authors: Umaru Barrie[1, 2], Katherine Floyd[1, #], Arani Datta[1], and Dawn M. Wetzel[1, 3*]

Affiliations: [1]Department of Pediatrics, University of Texas Southwestern Medical Center, 5323 Harry Hines Blvd, Dallas, Texas, 75390, United States; [2]Medical Scientist Training Program, University of Texas Southwestern Medical Center, 5323 Harry Hines Blvd, Dallas, Texas, 75390, United States; [3]Department of Biochemistry, University of Texas Southwestern Medical Center, 5323 Harry Hines Blvd, Dallas, Texas, 75390, United States.

*Corresponding author: Dawn M. Wetzel, M.D., Ph.D.
Departments of Pediatrics (Infectious Diseases) and Biochemistry
The University of Texas Southwestern Medical Center, Dallas, TX 75019
Phone: 214-645-9510; Email: Dawn.Wetzel@UTSouthwestern.edu

[#]**Current address:** Department of Internal Medicine and Molecular Microbiology, Washington University School of Medicine, 660 S Euclid Ave, St. Louis, MO 63110, United States

Author contributions: U.B. and D.M.W. designed and performed experiments, analyzed data, and wrote the manuscript. K.F. conducted experiments, assisted with data analysis, and edited the manuscript. A.D. helped to design and perform experiments, analyzed data, and edited the manuscript.

This file includes:

Abstract word count: 225

Lay summary word count: 141

Manuscript word count: 6236

Number of references: 63

Number of figures: 6

Number of tables: 2

Supplemental figures: 4

Supplemental tables: 3

ABSTRACT: The obligate intracellular protozoan parasite *Leishmania* binds several host cell receptors to trigger its uptake by phagocytic cells, ultimately resulting in visceral or cutaneous leishmaniasis. After *Leishmania* engages receptors on macrophages and other phagocytes, a series of signaling pathways in the host cell are activated during its internalization, which are critical for establishment and persistence of *Leishmania* infection. Thus, preventing *Leishmania* internalization by phagocytes could be a novel therapeutic strategy for leishmaniasis. However, the host cellular machinery that mediates promastigote and amastigote uptake is not well understood. Here, using small molecule inhibitors of Mitogen-activated protein kinases/Extracellular signal regulated kinases (MAPK/ERK), we demonstrate that ERK1/2 mediates *Leishmania amazonensis* uptake and (to a lesser extent) phagocytosis of beads by macrophages. We find that inhibition of MEK1/2 or ERK1/2 leads to inefficient amastigote uptake by macrophages. Moreover, using inhibitors and primary macrophages lacking spleen tyrosine kinase (SYK) or Abl family kinases, we show that SYK and Abl family kinases mediate Raf, MEK, and ERK1/2 activity and are necessary for efficient uptake. Finally, we demonstrate that trametinib, a MEK1/2 inhibitor used clinically to treat certain cancers, significantly reduces disease severity and parasite burden in *Leishmania*-infected mice, even if it is started significantly after lesions develop. Our results show that maximal *Leishmania* infection requires MAPK/ERK and highlight the potential for MAPK/ERK-mediated signaling pathways to be novel therapeutic targets for leishmaniasis.

Keywords: *Leishmania*, kinase, MAPK/ERK, parasite, macrophage

Abbreviations: BCA, Bicinchoninic acid; BMDM, bone marrow-derived macrophages; CC, cytotoxic concentration; CR3, complement receptor 3; FcγR, Fc gamma Receptor; h, hour; IC, inhibitory concentration; IL, Interleukin; INFγ, Interferon gamma; Mϕ, macrophage; m, minutes; MAPK/ERK, Mitogen-activated protein kinases/Extracellular signal regulated kinases; PKC, Protein Kinase C; PVDF, polyvinylidene difluoride; RAF, Rapidly Accelerated Fibrosarcoma; RIPA, radioimmunoprecipitation assay; p-, phosphorylated; PMA, Phorbol 12-myristate 13-acetate; SD, standard deviation; SFK, Src family kinases; SYK, spleen tyrosine kinase; TNF, Tumor Necrosis Factor

Lay summary: *Leishmania* is a single-celled parasite that causes skin ulcers or a disseminated disease in humans. Our goal is to identify new drugs to treat *Leishmania* infection. *Leishmania* must live inside human immune cells to cause disease. If *Leishmania* is not able to enter human immune cells, it dies. Our studies demonstrate how *Leishmania* infection permits a set of proteins called MAP kinases to pass signals from one protein to the next within mammalian immune cells. The resulting signals allow *Leishmania* to enter into these immune cells and survive within its host. Importantly, trametinib, a drug that prevents these signals from MAP kinases, decreases the development of skin ulcers when it is given to mice that are infected with *Leishmania*. Our findings suggest that

84 leishmaniasis could be treated with drugs that act on kinases found in humans

85 rather than the parasites themselves.

86

87 **One sentence summary**: An Abl2-SYK-Raf-MEK-ERK pathway facilitates

88 *Leishmania* uptake by phagocytic cells and promotes disease severity in

89 *Leishmania*-infected mice.

90

1. INTRODUCTION

Leishmania spp. are obligate intracellular, protozoan parasites spread by the sand fly vector [1], causing leishmaniasis, a group of diseases ranging from self-healing cutaneous ulcers [2] to deadly disseminated visceral disease [3]. Leishmaniasis represents a major global health problem, since over 12 million people currently suffer from this disease. Approximately 2 million people are newly infected by *Leishmania* spp. annually [4]. Moreover, over 350 million people in 98 countries worldwide are at risk of developing leishmaniasis [4, 5], and the disease is now spreading into previously non-endemic areas, including the United States [6, 7]. *Leishmania*, particularly the species causing cutaneous disease, are understudied, and current treatments are few, expensive, poorly effective, and toxic. Resistance is also emerging [8-11]. Thus, identifying new drugs with novel mechanisms of action that circumvent resistance mechanisms is an urgent priority for effective drug development.

When an infected sand fly encounters its host, *Leishmania* promastigotes must be internalized by phagocytic cells such as macrophages (Mϕ) to persist in the host [12, 13]. This process is then repeated as the mammalian life cycle stage, the amastigote, replicates and spreads to other phagocytic cells to cause pathogenesis [14]. Amastigotes that do not enter phagocytic cells are thought to be cleared by the host immune system and/or die from lack of essential nutrients [14]. Major advancements have been made in understanding the immunomodulatory events involved in the pathogenesis of leishmaniasis.

114 However, little is known about the basic molecular events underlying the
115 pathogenesis, especially the host cellular signaling pathways, which facilitate the
116 uptake of *Leishmania* by Mϕs and other phagocytes.
117
118 Based on prior studies, the Fcγ classes of receptors (FcγR) are the primary
119 receptors on the host cell surface that permit amastigote uptake [14], and the
120 complement receptor CR3 is the primary mediator of promastigote uptake [15].
121 Our previous studies have identified the Src [16] family kinases (SFK, and
122 specifically Hck, Fgr, and Lyn), Abl1 (Abl) and Abl2 (Arg) [17] kinases, and
123 Spleen Tyrosine Kinase (SYK) [18] as major protein families involved in
124 phagocytosis and *Leishmania* uptake. In particular, we have demonstrated that
125 Abl facilitates complement-mediated phagocytosis, and Arg enhances
126 immunoglobulin/ FcγR-mediated phagocytosis [16, 17]. Modulation of these
127 kinases via genetic manipulation or small molecule inhibitors abrogates *L.*
128 *amazonensis* internalization by Mϕs, and thus limits disease progression in mice
129 [16, 17]. However, our studies also indicate that these kinases have a limited role
130 in the host's immune response to *Leishmania* or parasite clearance [16, 17]. A
131 drug that simultaneously decreases parasite uptake and promotes host-
132 advantageous immunological responses could provide reductions in infection and
133 disease burden. Host-cell active agents also could be used to combat other
134 intracellular pathogens that employ similar uptake mechanisms.
135

136 Exactly how SFK, Abl family kinases, and SYK would regulate the events that
137 occur during *Leishmania* uptake and phagocytosis has not been fully established.
138 Others and we have demonstrated that CrkII is activated after signals have been
139 relayed from SFK to Arg to SYK, leading to actin-rich phagocytic cup formation
140 and pathogen uptake [16-19]. Interestingly, studies have been published
141 primarily in cancer model systems indicating that SFK [20], Abl family kinases
142 [20], and SYK [21, 22] also can activate MAPK/ERK signaling. MAPK/ERK are
143 known to directly phosphorylate cytoplasmic or nuclear proteins, including
144 transcription factors, that control several fundamental cellular processes from
145 proliferation and differentiation to innate and adaptive immune responses [23-25].
146 In addition, Phorbol 12-myristate 13-acetate (PMA) is known to activate
147 MAPK/ERK through protein kinase C (PKC) [26].
148
149 It is not clear whether MAPK/ERK signaling would mediate the uptake of
150 *Leishmania* parasites by phagocytes. Research on *Plasmodium* indicated that
151 inhibiting MEK1/2, which is upstream of ERK1/2, affects both adaptive and innate
152 immune responses, which limits parasitemia and prevents pathogenesis [27].
153 Previous studies have also shown that MAPK/ERK signaling modulates the
154 immune response to *L. amazonensis* infection to favor chronic infection, where
155 subversion of MAPK/ERK signaling leads to parasite survival inside phagocytic
156 cells, although these results vary depending on species [28-32].
157 Correspondingly, limiting MAPK activity using the older-generation MAPK
158 inhibitors PD98059 or U0126 has been shown to enhance *L. amazonensis* killing

159 by activating reactive oxygen species (ROS) and repressing IL-10 production
160 [33-36]. These results implicate ERK1/2 phosphorylation as a mechanism
161 through which *L. amazonensis* promotes persistence and subverts the immune
162 response [33]. However, experiments characterizing the role of MAPK/ERK
163 signaling during parasite uptake by Mϕ have not been conducted.
164
165 Here, we uncover an additional role for MAPK/ERK during *Leishmania*
166 internalization by phagocytes. We show that Raf-1, MEK1/2, and ERK1/2 activity are
167 necessary for efficient uptake of amastigotes. Host MAPK/ERK is activated by Arg
168 and SYK to facilitate this process. In combination with prior results [16, 17, 33], our
169 molecular studies elucidate an FcγR-SFK-Arg-SYK-Raf-MEK-ERK signaling relay as
170 a major pathway involved in establishment of leishmaniasis by facilitating parasite
171 uptake. In addition, using a mouse model, we establish that trametinib, a selective
172 MEK inhibitor that is clinically approved to treat cancer, decreases footpad swelling
173 and parasite burden in cutaneous leishmaniasis, even if it is started significantly after
174 lesions are apparent. Our experiments highlight MAPK/ERK inhibitors as potential
175 treatment modalities for this devastating disease.
176

177 **2. MATERIALS AND METHODS**

178 **2.1 Mice.** C57BL/6 mice were procured from Jackson Laboratory (Bar Harbor, ME).
179 *Syk*$^{flox/flox}$ *Cre*$^{+}$ and *Arg*$^{-/-}$*Abl*$^{flox/flox}$ *LysM Cre*$^{+}$ mice are either on a pure C57BL/6
180 background (SYK) [18] or have been backcrossed to C57BL/6 mice at least 5 times
181 (Abl/Arg) [16], [17]. All the experiments involving knockout mice were conducted with
182 WT littermates to ensure control for their genetic background. The Institutional
183 Animal Care and Use Committee at University of Texas Southwestern Medical
184 Center provided approval for all experimental protocols.

185

186 **2.2 Mammalian cell culture.** RAW 264.7 cells (ATCC, Manassas, VA) were
187 cultured in Dulbecco's modified Eagle's medium (DMEM) plus 10% endotoxin-free,
188 heat-inactivated, fetal bovine serum (FBS) (GeminiBio, Sacramento, CA) and 1%
189 penicillin–streptomycin as described previously [16]. FBS was checked for LPS
190 contamination using a highly sensitive Pierce™ Chromogenic Endotoxin Quant Kit
191 (Thermo Scientific, Cat No. A39552), and was found to be endotoxin negative (< 0.1
192 EU/ml). For experiments with bone marrow-derived Mϕs (BMDM), cells were
193 obtained from the humeri, tibias, and femurs of *WT, Syk*$^{flox/flox}$ *Cre*$^{+}$, or *Arg*$^{-/-}$*Abl*$^{flox/flox}$
194 *LysM-Cre*$^{+}$ mice. They were differentiated to *WT, Syk*$^{flox/flox}$ *Cre*$^{+}$, or *Arg*$^{-/-}$*Abl*$^{flox/flox}$
195 *LysM-Cre*$^{+}$ BMDM by culturing them in DMEM, 10% FBS, and 20% L929 cell
196 supernatant over 7 days. Differentiation to Mϕ was confirmed [17] and samples were
197 screened for *Mycoplasma* contamination [37].

198

199 **2.3 Parasite culture.** *L. amazonensis* promastigotes (strain IFLA/BR/67/PH8,
200 provided by Norma W. Andrews, University of Maryland, College Park, MD) were
201 maintained at 26°C in Schneider's Drosophila medium (Sigma, S9895, St. Louis,
202 MO) plus 15% FBS and 1% penicillin–streptomycin [16, 17]. *L. amazonensis*
203 amastigotes were grown axenically at 32°C in Schneider's Drosophila medium at
204 pH 5.5, plus 20% FBS, 1% penicillin–streptomycin, 0.1% hemin (25 mg/mL in
205 50% triethanolamine), 10 mM adenine, 5 mM L-glutamine, 0.25% glucose, 0.5%
206 trypticase, and 40 mM sodium succinate (all from Sigma) [16, 17]. For uptake
207 (internalization of amastigotes and promastigotes) assays, promastigotes were
208 incubated for 7 days to maximize infective metacyclics (*i.e.*, those isolated
209 through a step Percoll gradient; Sigma). Amastigotes typically were grown
210 axenically for 5 days prior to use [17]. To assess for amastigote growth and
211 replication defects during incubation in MEK/ERK activators or inhibitors, medium
212 containing 10 μM trametinib (Selleck Chemicals, Houston, TX), PMA (Selleck
213 Chemicals), or 0.1% dimethyl sulfoxide (DMSO, Sigma) was used. To ensure
214 infectivity, parasites were periodically passed in C57/BL6 mice prior to isolation
215 of amastigotes from footpad lesions.
216
217 For some experiments, a transgenic stable mNeonGreen expressing line of *L.*
218 *amazonensis* parasites (*L. amazonensis*-mNeon), containing a marker for
219 hygromycin resistance, was generated [18]. *L. amazonensis*-mNeon
220 promastigotes and amastigotes were maintained as above, but the media was
221 supplemented with 100 μg/mL hygromycin (Sigma). *L. amazonensis* virulence

222 was maintained by passage in C57BL/6 mice [17]. *L. amazonensis*-mNeonGreen
223 parasites were detected with an excitation wavelength of 490–494 nm and
224 emission of 515 nm.
225
226 **2.4 *Leishmania* uptake assays.** Experiments were adapted and modified as
227 described previously [16, 17]. BMDM (*WT, Syk*$^{flox/flox}$ *Cre*$^{+}$, *Arg*$^{-/-}$*Abl*$^{flox/flox}$ *LysM-Cre*$^{+}$)
228 or RAW 264.7 cells were plated and treated with inhibitors (imatinib [Arg/Abl
229 inhibitor], PD0325901 [MEK1/2 inhibitor], SCH772984 [ERK1/2 inhibitor], trametinib
230 [MEK1/2 inhibitor]) (Selleck Chemicals, Houston, TX), PMA [ERK1/2 activator] or
231 DMSO, where appropriate. Metacyclic promastigotes were incubated in fresh mouse
232 serum for C3bi opsonization, and amastigotes were coated with anti-P8-
233 proteoglycolipid complex (monoclonal antibody IgG1) [18]. Next, samples with RAW
234 264.7 cells or BMDMs were incubated with C3bi-opsonized promastigotes at 10
235 parasites to 1 Mϕ or with IgG-opsonized amastigotes at 10 parasites to 1 Mϕ for 2
236 hours (h), unless otherwise indicated, and fixed with 3% formaldehyde for 20
237 minutes (m). Mouse anti-gp46 antibody was allowed to bind to external
238 promastigotes, whereas mouse anti-P8 antibody was incubated with external
239 amastigotes, as described previously [16, 17]. Samples were then incubated with
240 Alexa-Fluor-568-conjugated donkey anti-mouse-IgG secondary antibody. Any
241 internalized parasite did not receive any antibody tagging and fluoresces green.
242 Conversely, external parasites are visualized in both the red and green channels
243 (orange in a merged image). All antibodies are listed in **Supplemental Table 3**.
244 Thus, this three-color immunofluorescence assay [18] allowed distinguishing of

245 internal (green) and external *L. amazonensis* promastigotes or amastigotes (green +
246 red).
247
248 For quantification, samples were imaged with a BioTek Cytation 5 (Agilent, Santa
249 Clara, CA) confocal imaging reader using a 40x objective lens with automated
250 analysis performed [16]. At least 16 randomly selected fields were automatically
251 visualized per well with each field assessing the number of Mϕs and amastigotes or
252 promastigotes (internalized versus external). The absolute phagocytic index (the
253 number of internalized amastigotes or promastigotes per 100 Mϕs) and adhesion
254 index (the total number of amastigotes or promastigotes per 100 Mϕs) was
255 calculated for each condition. The absolute phagocytic index or adhesion index for
256 DMSO-treated conditions (control) was taken as the maximum value (100%) for
257 each experiment, and the phagocytic index for imatinib, SCH772984, trametinib, or
258 PMA-treated samples was determined and normalized relative to that of the control.
259 Means ± SD were calculated. Each experiment was performed with at least 3
260 biological repeats and contained 3 technical replicates. A one-sample Student's *t*-
261 test or two-way ANOVA was used to determine statistical significance, where
262 appropriate. The representative images shown were visualized using a Biotek
263 Cytation 5 imaging multimode reader. Parasites in representative images were
264 selected from files and linearly processed in Adobe Photoshop CS6 (version 13.0.6).
265 Where applicable, permeabilized samples were labeled with far-red phalloidin
266 (A22287, Thermo Fisher Scientific) at 1:100. For phagocytic cup analysis and
267 representative images, data were collected on a Zeiss LSM 880 inverted confocal

268 Airyscan microscope at 40X (analysis) or 63X (representative images). Images were
269 created via Image J (1.52a, http://imagej.nih.gov/ij) and processed in Adobe
270 Photoshop 13.0.6. [38].
271
272 **2.5 Phagocytosis of beads.** Experiments were adapted and modified as described
273 previously [16, 17]. RAW 264.7 cells were plated at 70% confluence and incubated
274 overnight in serum-free medium. Except where indicated, samples were pre-
275 incubated in medium containing 3.3 μM imatinib, 1 μM SCH772984, 1 μM trametinib,
276 250 nM PMA or 0.1% DMSO for 1-2 h. Next, latex yellow–green 2 μm beads
277 (Sigma) were coated with human IgM (Sigma, Cat. #: I-8260) and incubated in rabbit
278 anti-IgM (Sigma, Cat. #: 270A) for IgG opsonization (confirmed as described
279 previously [17]). Mϕs were incubated with 10–15 beads/ Mϕ for 2 h, unless otherwise
280 stated, at 37°C. They were fixed with 3% formaldehyde for 20 m, blocked using 2%
281 BSA in PBS (no permeabilization), and then incubated with rabbit anti-human IgM
282 and Hoechst 33258 dye (Sigma) to visualize nuclei. Next, samples were incubated
283 with an Alexa-Fluor-568-conjugated goat anti-rabbit-IgG secondary antibody
284 (Invitrogen, Cat.#: A11034). All antibodies are listed in **Supplemental Table 3**. This
285 multi-color immunofluorescence assay [39] allowed distinguishing of internalized
286 (green) and external beads (green + red), similar to described above for internal vs
287 external *L. amazonensis*. Quantification was done as above with a BioTek Cytation 5
288 confocal imaging reader using a 40x objective lens with automated analysis
289 performed by the Cytation 5.
290

291 **2.6 Western Blot**. To analyze protein/phosphoprotein expression, western blotting
292 was performed. Briefly, RAW 264.7 cells or BMDMs from *WT, Syk*$^{flox/flox}$ *Cre*$^{+}$, or
293 *Arg*$^{-/-}$*Abl*$^{flox/flox}$ *LysM-Cre*$^{+}$ mice were incubated overnight in serum-free media (RAW
294 264.7 cells) or L929-free media (BMDM). Experiments were performed at ~70%
295 confluence. Where appropriate, Mϕ were pre-incubated in imatinib, entospletinib,
296 PD0325901, selumetinib, SCH772984, trametinib, PMA or DMSO. IgG-opsonized
297 amastigotes or IgG-opsonized beads were added to adherent starved Mϕs for 30 m,
298 unless otherwise indicated [40], and cells lysed with RIPA extraction buffer and halt
299 protease and phosphatase inhibitor (Thermo Scientific, Cat. #: 78440, Richardson,
300 TX). Protein purity and concentration were addressed using Coomassie Blue
301 staining and BCA assay, respectively, following the manufacturers' protocols. Total
302 proteins were resolved by polyacrylamide gel electrophoresis (12% gels) and
303 transferred to PVDF membranes (BioRad). The membranes were blocked in 5%
304 non-fat dry milk in Tris-buffered saline (TBS) (20 mM Tris at pH 7.6, 150 mM NaCl).
305 The membrane was incubated overnight at 4˚C with the primary antibody in 5% BSA
306 and TBS-T. Next, horseradish peroxidase (HRP)-conjugated anti-mouse secondary
307 antibody (#7076, Cell Signaling Technology) was added at 1:5000 in 5% non-fat dry
308 milk in TBS-T for 1 h. All antibodies are provided in **Supplemental Table 3**.
309 Membranes were incubated in SuperSignal West Pico Chemiluminescent Substrate
310 (Thermo Scientific) for 5 m and visualized by using a phosphorimager (ImageQuant
311 LAS 4000, GE Healthcare). For analysis, relative amounts of phosphorylated
312 proteins were compared to total proteins with ImageJ analysis software
313 (https://imagej.nih.gov/ij); membranes were stripped and reprobed). Each

314 experiment had at least 3 biological replicates. Two-way ANOVA was used for
315 statistical tests.
316
317 **2.7 *Leishmania* animal model.** For the mouse footpad model of cutaneous
318 leishmaniasis, 10 female C57BL/6 mice per group were infected between 6 and 8
319 weeks (w) of age as previously described [16, 17]. Briefly, 1×10^6 metacyclic
320 promastigotes were suspended in PBS and injected subcutaneously in the dorsal
321 side of the right hind foot. For the experiments in Fig 6A-C, mice were provided 2
322 mg/kg body weight of trametinib or drug vehicle (4% DMSO and 1% corn oil) by oral
323 gavage daily starting a w before infection and continuing until the mice were
324 euthanized. Two independent experiments were performed. For the experiments in
325 Fig 6D-F, mice were provided 2 mg/kg body weight of trametinib or drug vehicle by
326 oral gavage daily starting 6 w after infection and continuing until the mice were
327 euthanized. Two independent experiments were performed. Lesion growth was
328 documented with calipers every other w by an investigator who was blinded to
329 condition. The ratio of the infected: uninfected foot size was obtained [41]. ANOVA
330 was used to compare diluent and trametinib-treated mouse groups to swelling at
331 time 0. The number of parasites in lesions was determined by limiting dilution upon
332 termination of the experiment between w 14 to 16 [42].
333
334 Lymph nodes from infected diluent versus trametinib-treated mice were obtained for
335 cytokine and chemokine profiling [42, 43]. Briefly, lymph node cells were incubated
336 in RPMI 1640 (Invitrogen) plus 10% heat-inactivated FBS, 5×10^{-5} M 2-

337 mercaptoethanol (Sigma), and 1% penicillin-streptomycin. Cells were stimulated with
338 promastigote lysates (equivalent to 1×10^6 or 1×10^5 parasites per sample, as
339 indicated) or concanavalin A (ConA) (5 μg/ml; Sigma). Supernatants were harvested
340 at 72 h and the levels of the cytokines and chemokines IL-4, IL-10, IL-12, IL-13, IL-
341 17, IFN-γ, IL-1β, IL-1α, IP-10, MIP-1α (CCL3), MIP-2 (CXCL2), CXCL9, RANTES
342 (CCL5), and MIP-1β (CCL4) were profiled using the custom multiplex Luminex
343 Platform (R&D Systems, Inc, Minneapolis, MN) through the UT Southwestern
344 Microarray Core as described previously [44, 45]. Background cytokine levels were
345 calculated using unstimulated supernatants.
346

347 **3. RESULTS**

348 **3.1 MAPK/ERK signaling in Mϕ facilitates *Leishmania* uptake**

349 To directly test whether the MAPK/ERK pathway mediates *Leishmania* uptake,
350 we first explored the effect of the MEK1/2 inhibitor trametinib on the uptake of *L.*
351 *amazonensis*. We can grow both promastigotes and amastigotes of this species
352 in tissue culture without host cells (*i.e.*, axenic culture), which facilitates our
353 studies of *Leishmania* uptake by Mϕs. Trametinib is a highly selective and potent
354 MEK1/2 inhibitor, with an IC_{50} for the purified kinase ranging from 0.92 nM to 3.4
355 nM in cell-free assays [46, 47]. Trametinib has no effect on the kinase activity of
356 c-Raf, B-Raf, or ERK1/2. We pretreated RAW 264.7 cells, a Mϕ–like cell line, for
357 2 hours (h) with trametinib or imatinib, an Abl/Arg inhibitor with an IC_{50} of 100-500
358 nM in kinase assays [35], as a positive control. We then added *Leishmania* to
359 samples to allow uptake and processed for immunofluorescence microscopy.
360 Visually, trametinib decreased the uptake of IgG-opsonized amastigotes in RAW
361 264.7 cells, comparable to the reductions seen after treatment with imatinib (**Fig.**
362 **1A).** Defects in internalization were quantified by calculating the phagocytic index
363 (PI), or number of internalized parasites per 100 Mϕ, which was lower in
364 trametinib-treated samples (**Fig. 1B**). No differences were seen in the total
365 (external + internal) number of *Leishmania* per 100 RAW 264.7 cells, which is
366 termed an adhesion index, among these conditions (**Fig. 1C**). We performed a
367 titration of trametinib's effects on amastigote uptake, and the maximal reduction
368 in PI was shown at 1 μM trametinib (**Fig. 1D, E**)**.** We also determined that over
369 72 h, the CC_{50} (cytotoxic concentration required to kill 50% of viable cells) for

370 RAW 264.7 cells was greater than our maximum concentration of 2.5 μM.
371 Internalization defects remained even after prolonged incubation in trametinib (up
372 to 240 minutes, m) and were not due to reduced adhesion, as amastigotes
373 continued to be bound to trametinib-treated RAW 264.7 cells at levels
374 indistinguishable from controls (**Fig. 1F, G**). Treating Mϕs with other MAPK/ERK
375 pathway inhibitors [48] such as selumetinib and PD0325901 (MEK1/2 inhibitors),
376 as well as SCH772984 (an ERK1/2 inhibitor), also significantly reduced
377 amastigote uptake without affecting the total number of bound parasites
378 (**Supplemental Fig. 1A, B**). In addition, we found that treating RAW 264.7 cells
379 with the MEK1/2 inhibitor PD0325901 [49] decreased the internalization of
380 promastigotes to a degree that was comparable to imatinib (**Supplemental Fig.**
381 **1C, D**). Next, we characterized growth curves and found that trametinib showed
382 no impact on cell viability and motility of parasites in culture (**Fig. 1H**). Together,
383 these similar results using multiple MAPK/ERK inhibitors establish that targeting
384 MEK1/2 and ERK1/2 significantly attenuates internalization of both *L.*
385 *amazonensis* life cycle stages. In addition, as previously published for
386 MAPK/ERK inhibitors, amastigotes within Mϕs had a ~50% reduction in survival
387 when cultures were treated with trametinib for 72 h (**Supplemental Fig. 1E**).
388

389 **3.2 cRaf, MEK1/2, and ERK1/2 are activated during amastigote uptake**

390 Having established that MAPK/ERK are important for *Leishmania* uptake, we
391 assessed whether kinases in this pathway were activated in host cells during
392 amastigote internalization. Raf-1 (cRaf), MEK1/2, and ERK1/2 are key members of

393 the MAPK/ERK pathway [25, 50]. We thus measured cRaf, MEK1/2, and ERK1/2
394 phosphorylation in RAW 264.7 cells to examine the relative phosphorylation level of
395 each kinase during internalization of amastigotes. Essentially no phosphorylated
396 ERK or ERK was detected in amastigote samples (**Supplemental Fig. 2A**).
397 However, amastigotes potently induced ERK1/2 phosphorylation in Mϕs, with
398 phosphorylation levels increasing by 3 and 4.5-fold at 10 and 30 m post-infection,
399 respectively (**Fig. 2A**). Similarly, MEK1/2 (**Fig. 2B**) and cRaf (**Fig. 2C**) were
400 activated by amastigotes that were entering host cells**.** These data indicate that
401 amastigotes rapidly activate MAPK/ERK in a sustained fashion during their uptake
402 by Mϕs.
403
404 **3.3 PMA rescues MAPK/ERK related uptake defects**
405 PMA is known to activate ERK1/2 through PKC, with an IC_{50} of 11.7 nM against
406 purified kinase [26]. Consistent with this, although PKC activation was seen during
407 the uptake of amastigotes, PMA treatment increased PKC phosphorylation in RAW
408 264.7 cells to 8-fold higher levels (**Fig. 3A, B**). Importantly, 10 μM PMA did not affect
409 growth of amastigotes in culture (**Fig. 3C**), indicating that it does not act directly on
410 *Leishmania*. We next investigated whether PMA affected amastigote internalization.
411 To perform these experiments, and to confirm our prior results from a cell line using
412 primary cells, we isolated bone marrow derived-Mϕs (BMDM) from C57BL/6 mice.
413 PMA-treated BMDM were able to internalize IgG-coated amastigotes at higher levels
414 than DMSO-treated BMDM in a dose-dependent manner, reaching maximal
415 internalization at 2.5 μM PMA (**Fig. 3D-F**). Furthermore, PMA treatment rescued

416 trametinib inhibition of *Leishmania* uptake in BMDM to PI that were indistinguishable
417 from those of DMSO-treated controls (**Fig. 3G, H**). Collectively, our data indicate that
418 ERK1/2 kinase activity is necessary for maximal *Leishmania* uptake.
419
420 **3.4 ERK1/2 is activated by Arg/Abl and SYK during amastigote uptake**
421 Next, we investigated the mechanism by which *L. amazonensis* amastigotes induced
422 ERK1/2 phosphorylation during their uptake. Previous research has shown that Arg
423 facilitates *Leishmania* amastigote uptake downstream of SFK [16]. In addition,
424 inhibition of SYK, a tyrosine kinase implicated in FcγR immunoglobulin-mediated
425 signaling [18, 33, 51, 52] reduces ERK1/2 activation in a dose-dependent manner in
426 other systems [18, 33]. To test for roles for these kinases, small molecule inhibitors
427 (imatinib, entospletinib [IC_{50} for activity against purified SYK = 7.7 nM] [18],
428 SCH772984, trametinib), and PMA were added to RAW 264.7 cells before infection
429 with amastigotes. Inhibition of Arg and SYK with imatinib and entospletinib,
430 respectively, significantly reduced ERK1/2 phosphorylation, to a similar degree to
431 the MAPK/ERK inhibitors SCH772984 and trametinib (**Fig. 4A, B**). As expected,
432 PMA, the positive control, significantly increased ERK1/2 phosphorylation (**Fig. 4A,**
433 **B**). The inhibitors and activators followed similar trends for promastigote-induced
434 ERK activity (**Supplemental Fig. 2B**). Thus, we could modulate *Leishmania*-induced
435 ERK activity by both inhibitors and activators *in vitro*.
436
437 To further characterize the role of SYK and Arg in *Leishmania*-induced ERK
438 phosphorylation, we next isolated BMDM from mice lacking Abl family kinases

439 (*Arg*$^{-/-}$*Abl*$^{flox/flox}$*LysM Cre*$^{+}$ [hereafter termed *Arg*$^{-/-}$*Abl*$^{-/-}$ when discussing isolated
440 BMDM]), SYK (*SYK*$^{flox/flox}$ *Cre*$^{+}$, abbreviated *SYK*$^{-/-}$ when referring to isolated BMDM)
441 or wild type (*WT*) littermates. We have previously shown that amastigote uptake is
442 dependent upon Arg but not Abl [15-16]. Our immunoblots showed *Arg*$^{-/-}$*Abl*$^{-/-}$ and
443 *SYK*$^{-/-}$ BMDM nearly completely lack Arg or SYK, respectively, while ERK1/2
444 expression was maintained (**Supplemental Fig. 2C**). Consistent with our chemical
445 inhibition experiments, *SYK*$^{-/-}$ and *Arg*$^{-/-}$*Abl*$^{-/-}$ BMDM limited amastigote-mediated
446 ERK1/2 phosphorylation, demonstrating that SYK and Arg/Abl are necessary for
447 stimulating ERK1/2 phosphorylation following engagement of the FcγR (**Fig. 4C, D**).
448 At low doses (250 nM), PMA rescued ERK1/2 activity in *Arg*$^{-/-}$*Abl*$^{-/-}$ and *SYK*$^{-/-}$
449 BMDM. This suggested 1) amastigotes operate through a distinct pathway to
450 activate ERK1/2 compared to PMA, which activates MAPK/ERK through PKC [26]
451 and 2) during FcγR-mediated amastigote infection, Arg and SYK family kinases are
452 upstream of MAPK/ERK and are necessary to activate the MAPK/ERK pathway.
453
454 To directly test whether Abl family kinases are critical for ERK1/2-mediated
455 amastigote uptake, we treated *WT* and *Arg*$^{-/-}$*Abl*$^{-/-}$ BMDM with DMSO or PMA prior
456 to infection with IgG-opsonized amastigotes. We found that *Arg*$^{-/-}$ *Abl*$^{-/-}$ BMDM
457 displayed defects in IgG-mediated amastigote uptake, while PMA treatment partially
458 rescued these defects (**Fig. 4E-G**), returning uptake to 66.4 ± 16.6% (mean ± SD)
459 compared to 29.3 ± 0.9% with DMSO. Similarly, SYK was necessary for efficient
460 amastigote uptake, and the decreased PI of *SYK*$^{-/-}$ BMDM was partially rescued by
461 PMA treatment (**Supplemental Fig. 2D, E)**. Taken together, these results, in

462 combination with prior data, are consistent with a signaling pathway in which Arg/Abl
463 and SYK act upstream of and activate the ERK1/2 pathway (which is at least partly
464 independent from PKC) to facilitate amastigote uptake [26].
465
466 **3.5 MAPK/ERK inhibition minimally impacts phagocytosis of opsonized beads**
467 *Arg*$^{-/-}$ BMDM have been shown to have impaired FcR-mediated phagocytosis
468 overall, as demonstrated using IgG-coated (opsonized) beads [17]. Thus, we
469 hypothesized that the Arg-SYK-ERK pathway may be necessary for the general
470 process of phagocytosis, in addition to amastigote uptake. To delineate the specific
471 contributions of MAPK/ERK to phagocytosis, we examined bead uptake compared
472 to amastigote uptake by RAW 264.7 cells. Surprisingly, phagocytosis of IgG-
473 opsonized beads by RAW 264.7 cells was minimally affected by trametinib (**Fig. 5A,**
474 **B**) or SCH772984 (**Supplemental Fig. 3),** both of which resulted in only a ~30%
475 reduction in uptake. Conversely, the uptake of IgG-coated amastigotes (**Fig. 1)** was
476 reduced by ~70% with trametinib treatment. However, when RAW 264.7 cells were
477 treated with imatinib, similar decreases in phagocytosis of IgG-opsonized beads
478 versus amastigotes were observed. These results suggest that Arg/Abl play a more
479 generalized role in phagocytosis, as we have demonstrated previously [17].
480 Collectively, our data suggest that ERK1/2 activation is important for *Leishmania*
481 uptake specifically but may play a minor role in standard phagocytic mechanisms.
482
483 We also tested whether MAPK/ERK activity was induced following addition of beads
484 compared to amastigotes. Beads induced ERK1/2 phosphorylation, but to levels that

485 were lower than in seen during amastigote uptake (**Fig. 5C, D**). This phosphorylation
486 occurred in a time-dependent fashion, such that activation reached maximal levels
487 between 5 and 10 m, and ERK1/2 phosphorylation was not detectable after 30 m
488 (**Fig. 5C, D**). Similarly, beads activated upstream kinases MEK1/2 (**Fig. 5E, F)** and
489 cRaf (**Fig. 5G, H**); however, their phosphorylation was not sustained. Thus, in
490 contrast to the sustained activation of MAPK/ERK that we saw during amastigote
491 uptake, beads had only a transient effect on ERK1/2 activation.
492
493 **3.6 Trametinib increases the intensity of actin labeled in phagocytic cups.**
494 Next, we explored the mechanisms by which trametinib affected *Leishmania*
495 amastigote internalization. We first characterized trametinib's effects on phagocytic
496 cup formation by performing an internalization assay with amastigotes as described
497 above, with the addition of fluorescent phalloidin to label phagocytic cups. We found
498 that phalloidin labeling around internalizing parasites was significantly brighter in
499 trametinib-treated Mϕs on average than DMSO-treated Mϕs, suggesting direct
500 effects on actin polymerization during the formation of actin-rich phagocytic cups
501 (**Supplemental Fig. 4A-C**). We next calculated the percentages of Mϕs infected by
502 amastigotes and the average numbers of amastigotes per infected Mϕ. We found
503 that both were affected by trametinib at approximately the values expected from the
504 decrease in phagocytic indexes (**Supplemental Fig. 4D-E**).
505
506 **3.7 Trametinib decreases lesion size and parasite burden in a murine model of**
507 **cutaneous leishmaniasis.** To test whether the MAPK/ERK pathway is necessary

508 for *Leishmania* pathogenesis *in vivo*, we employed a C57BL/6 mouse model of
509 cutaneous leishmaniasis using *L. amazonensis.* Footpad swelling (*i.e*., lesion size)
510 was measured in infected mice treated with 2 mg/kg of body weight/day of oral
511 trametinib or drug vehicle (control) starting 7 days (d) before inoculation and
512 continuing for the experimental duration of 14-16 weeks (w) [16, 17] (**Fig. 6A**).
513 Compared to controls, trametinib-treated mice developed smaller lesions (**Fig. 6B**),
514 which contained fewer parasites in lesions (**Fig. 6C**). The decreased number of
515 parasites found within lesions may help to explain these changes in lesion size.
516
517 Overall, in leishmaniasis, as a simplified paradigm, a Th1 response is thought to
518 be beneficial to the host, while a Th2 response is typically considered to be
519 deleterious. To determine whether the immunological effects of MEK1/2 inhibition
520 were associated with the healing seen in trametinib-treated mice, we isolated
521 draining lymph nodes from infected DMSO and trametinib-treated mice. We then
522 profiled cytokine and chemokine secretion after stimulation with high (1×10^6) or
523 low (1×10^5) doses of *L. amazonensis* lysates compared to unstimulated. A mild
524 shift in the overall ratio of Th1 to Th2 cytokines (Th1/Th2) towards a Th2
525 phenotype in trametinib-treated mice was seen (**Table 1**). Notably, lymph nodes
526 extracted from trametinib-treated mice released lower quantities of nearly all
527 cytokines in response to *L. amazonensis* than those isolated from diluent-treated
528 animals (**Table 2**). Trametinib-treated mice also demonstrated decreased
529 cytokine production in response to concanavalin A (Con A) stimulation. In
530 addition, we assessed chemokine secretion following MEK1/2 inhibition. The

531 production of several chemokines implicated in *Leishmania* pathogenesis,
532 including MIP-1α (CCL3) and MCP-1 (CCL2), were significantly decreased with
533 trametinib (**Table 2**), consistent with the decrease in cytokines/chemokines
534 overall.
535
536 We further tested whether MEK1/2 inhibition with trametinib reduces pathogenesis
537 after the development of symptoms by infecting mice as above. However, we started
538 diluent vs trametinib at 6 w after inoculation (*i.e.*, once lesions were clearly visible)
539 and continued therapy for the remaining experimental duration (**Fig. 6D**). Even with
540 this delayed treatment, trametinib-treated mice reproducibly had smaller lesions
541 (**Fig. 6E**). They also had significantly lower parasite burdens than those of controls
542 (**Fig. 6F**), which at least in part may explain these results. We also saw similar
543 immunological responses in mice treated with trametinib initiated partway through
544 the experiment as we did for the mice treated prior to *Leishmania* infection
545 (**Supplemental Table 1, Supplemental Table 2**) [53, 54]. Overall, our findings
546 demonstrate that trametinib administration limits the manifestations of leishmaniasis
547 in a mouse model, even if it is started after lesions have developed.

548 **4. DISCUSSION**

549 Here, we have shown that efficient *Leishmania* uptake by Mϕs and infection in mice
550 requires MAPK/ERK. While previous studies have shown that ERK1/2 activation
551 post-infection by *Leishmania* alters various host signaling pathways, leading to
552 increased intracellular survival and replication of these parasites [36, 55], our results
553 establish an earlier role for host ERK1/2 activity during the *Leishmania* life cycle, and
554 show that ERK1/2 is necessary for efficient *Leishmania* uptake into Mϕs.
555 Furthermore, our results delineate new activators of ERK signaling, and suggest that
556 MAPK/ERK affects actin polymerization. In combination with prior data, we propose
557 a model whereby, following engagement of the FcγR, host Arg/Abl and SYK
558 stimulate Raf, MEK, and ERK1/2 phosphorylation, leading to amastigote uptake
559 (**Fig. 6G**). Moreover, *in vivo* inhibition of MEK1/2 by trametinib in a mouse model of
560 cutaneous leishmaniasis significantly limits lesion development and parasite burden,
561 even when trametinib is started after these lesions have developed. Our results
562 highlight a critical role for MAPK/ERK signaling in *Leishmania* uptake and further
563 previously published studies of its role in the pathogenesis of leishmaniasis.
564

565 Our data indicate that Arg/Abl and SYK are required for amastigote-mediated
566 ERK1/2 phosphorylation following FcγR activation, which has not been
567 demonstrated previously. Our prior studies of host signaling required for *Leishmania*
568 uptake revealed that amastigotes bind directly to FcγR [15] and activate SFK-Arg
569 pathways [16] to induce uptake. We conclude from our combined results that an
570 FcγR-SFK-Arg-SYK signaling pathway functions upstream of and activates

571 MAPK/ERK family kinases, which in turn affects the amount of polymerized actin in
572 phagocytic cups. We previously published similar effects on actin polymerization
573 using the SYK inhibitor entospletinib during *Leishmania* uptake [18]. Interestingly,
574 pharmacological inhibition of MEK1/2 and ERK1/2 in RAW 264.7 cells significantly
575 reduce, but does not completely abolish, *Leishmania* uptake. One explanation for
576 these results is that kinase inhibition via these compounds may be incomplete.
577 Another is that *Leishmania* uptake may be mediated via additional host signaling
578 pathways. Supporting the latter hypothesis, we find that low or sub-EC_{50} doses of
579 PMA, which activates ERK1/2 through an SFK-Arg-SYK-independent manner,
580 rescues trametinib inhibition of *Leishmania* amastigote uptake in RAW 264.7 cells,
581 as well as in *SYK*$^{-/-}$ and *Arg*$^{-/-}$*Abl*$^{-/-}$ BMDM. PMA is a known activator of PKC [26,
582 56-60]. However, we find that PKC activity is only slightly increased during
583 amastigote infection of WT/DMSO-treated Mϕs, suggesting that PKC may play only
584 a minor role during typical amastigote uptake. Ongoing work in the laboratory is
585 directed at uncovering additional novel uptake mechanisms for *Leishmania*. In
586 addition, although drug combinations typically are not used to treat leishmaniasis,
587 they are the standard of care for many other infections, such as HIV or tuberculosis.
588 Combination therapy with multiple kinase inhibitors to inhibit several uptake
589 modulators at once may provide additional benefit for the treatment of leishmaniasis
590 over single host cell kinase inhibitors alone.
591
592 Our data using MEK/ERK inhibitors indicate that there are differences in MAPK/ERK
593 signaling within Mϕs depending on whether *Leishmania* amastigotes or IgG-coated

594 beads are undergoing internalization. These results differ from most available
595 literature that concludes that *Leishmania* primarily hijacks ongoing phagocytic
596 pathways to facilitate its uptake. We instead suggest that there may be alternative,
597 perhaps partly redundant, pathways that may support the uptake of *Leishmania* over
598 the phagocytosis of beads, and vice versa. Our future experiments will continue to
599 compare and contrast the signaling pathways required for these different uptake
600 mechanisms between opsonized beads and *Leishmania* parasites.
601
602 Our experiments using a mouse model for *Leishmania* infection, in combination with
603 prior studies [33], show that MAPK/ERK are required for maximal *Leishmania*
604 pathogenesis during cutaneous leishmaniasis. One highly plausible explanation for
605 the decreased lesion size and parasite burden that we see in trametinib-treated mice
606 is our previously documented inhibition of *Leishmania* uptake, in combination with
607 previous studies suggesting MAPK/ERK signaling affects parasite survival in Mϕs
608 [26-33]. Consistent with this hypothesis, fewer parasites are found in lesions from
609 trametinib-treated mice than in control mice. Alternately, lesion size variations after
610 *L. amazonensis* infection might result from known trametinib limitation of host
611 inflammatory and immunological responses. Many pathogens hinder immune
612 responses by targeting host intracellular signaling pathways, including MAPK
613 pathways [59, 61]; and MAPKs have been shown to play roles in the immune
614 response to leishmaniasis [26-33]. The murine immune response to leishmaniasis is
615 complicated and varies depending on the species of *Leishmania* and the mouse
616 strain used. As a simplified paradigm, Th1 responses are generally protective, but

617 Th2 responses are harmful to the host [28, 31, 32]. We find that all cytokines
618 assessed following *Leishmania* antigen stimulation in lymph nodes isolated from
619 infected trametinib-treated mice are reduced from the levels seen in diluent-treated
620 mice, similar to our prior results using bosutinib [16]. One possible explanation is that
621 fewer cytokines are generated because the lesions contain fewer parasites. Another
622 is that trametinib could instead dampen pathways important for maintaining an active
623 inflammatory response to the ongoing host response to infection. Supporting this
624 second possibility, cytokines measured after Con A stimulation (an antigen-
625 independent mitogen used as an alternative T cell stimulus) are significantly reduced
626 by MEK1/2 inhibition. Overall, the moderate shift in the total ratio of Th1 to Th2
627 cytokines (Th1/Th2) toward a Th2 phenotype that we see theoretically should
628 exacerbate disease rather than alleviate it. Reduced levels of proinflammatory
629 chemokines like MIP-1 (CCL3) and MCP-1 (CCL2), on the other hand, may be
630 responsible for reducing lesion size by restricting the number of immune cells,
631 especially phagocytic cells, which reach the site of infection. We do note a
632 surprisingly strong IL-10 response in the trametinib-treated mice, considering that
633 ERK activation has been shown to be required for IL-10 production by *Leishmania*-
634 infected Mϕs [62]. However, others have found that trametinib treatment increases
635 IL-10 production in mouse tissues [63]. Further work is needed to delineate the
636 regulation of immune responses to *Leishmania* infection and the resulting effects on
637 lesion worsening versus healing.
638

639 Finally, and of particular interest, we have demonstrated that there are reductions
640 in lesion size and parasite burden if trametinib is used in a *L. amazonensis*
641 mouse model of cutaneous leishmaniasis, even if it is started after foot swelling
642 has developed. Compared to our previous results, the data shown here strongly
643 suggest that trametinib is more effective for reducing lesion size than imatinib
644 [17] or bosutinib [16], which target signaling molecules in the same pathway.
645 Trametinib is used clinically to treat several cancers, making it feasible that this
646 drug could be repurposed to treat an infectious disease, and facilitating potential
647 clinical trials for its use against leishmaniasis. Our data imply that inhibiting a
648 signaling pathway downstream of SFK-Arg-SYK might improve results over
649 inhibiting kinases upstream in the pathway. Our results also give credence to our
650 overarching hypothesis that targeting host cell pathways, particularly ones that
651 are required for multiple aspects of the parasite life cycle and pathogenesis, may
652 permit treatment of an infectious disease such as leishmaniasis.
653

654 **5. CONCLUSIONS**

655 In summary, we have demonstrated that Arg-SYK signaling through MAPK/ERK
656 facilitates *Leishmania* uptake by Mϕ. Furthermore, ERK activity helps govern the
657 subsequent pathogenesis and disease progression of leishmaniasis in the mouse
658 model. Due to the relative specificity of newer-generation MAPK/ERK small
659 molecule inhibitors like trametinib, it is possible to selectively target MEK1/2 and
660 ERK1/2 for potential therapeutic intervention. Our findings demonstrate the
661 significance of MAPK/ERK signaling during *Leishmania* entry into phagocytic cells.

662 Our future studies will investigate the use of host-cell-active drugs, potentially in
663 conjunction with other kinase inhibitors or existing antiparasitics, to improve efficacy,
664 decrease toxicity, and limit the likelihood of developing resistance. Although
665 trametinib is not completely without side effects, this combination strategy could be
666 used to mitigate any risk of toxicity arising due to targeting essential signaling
667 pathways. Furthermore, our results support the novel possibility that medications
668 that target conserved host cell processes rather than infectious pathogens might be
669 employed to treat a wide spectrum of intracellular pathogens.
670

671 **6. ACKNOWLEDGEMENTS**

672 **6.1 Overview.** We thank Drs. Neal M. Alto, Melanie H. Cobb, Margaret A.
673 Phillips, James J. Collins, and Michael L. Reese (all at UT Southwestern) for
674 helpful discussions and feedback. Members of the UT Southwestern
675 Departments of Pediatrics, Biochemistry, Microbiology, and Pharmacology
676 provided valuable feedback and permitted common equipment use. Francis
677 Khuong and Catherine Trice provided expert technical assistance and helped to
678 edit this manuscript. Dr. Diane McMahon-Pratt (Yale University) generously
679 donated antileishmanial antibodies. Dr. Anthony J. Koleske (Yale University)
680 provided the *Arg*$^{-/-}$*Abl*$^{flox/flox}$ mice. The UT Southwestern Microarray Core
681 facilitated cytokine/chemokine profiling, the High Throughput Screening Core
682 assisted with data visualization and quantification, and the Live Cell Imaging
683 Core helped us with collecting confocal microscopy images.

684

685 **6.2 Funding.** This work was supported by a Children's Clinical Research
686 Advisory Committee (CCRAC) Junior Investigator Award, a CCRAC Early
687 Investigator Award, the National Institutes of Health (K08 AI103036 and R01
688 AI146349), Welch Foundation Grant I-2048, and the UT Southwestern
689 Department of Pediatrics (to D.M.W.). U.B. was supported by a National
690 Institutes of Health Supplement to Promote Diversity in Health-Related Research
691 (R01 AI146349- S1) and Medical Scientist Training (MD/PhD) Grant NIH
692 T32GM008014. K.F. was supported by a UT Southwestern-Amgen Summer
693 Research Fellowship.

6.3 Competing interests. The authors have no competing financial interests.

6.4 Data and materials availability. All data are available within the main text of the manuscript or the supplemental materials. Any materials generated for this manuscript are freely available upon request.

700 **7. REFERENCES AND NOTES**

701 1. Gossage SM, Rogers ME, Bates PA. Two separate growth phases during the
702 development of Leishmania in sand flies: implications for understanding the life cycle. Int
703 J Parasitol. 2003;33(10):1027-34. doi: 10.1016/s0020-7519(03)00142-5. PubMed PMID:
704 13129524; PubMed Central PMCID: PMCPMC2839921.

705 2. Markle WH, Makhoul K. Cutaneous leishmaniasis: recognition and treatment. Am
706 Fam Physician. 2004;69(6):1455-60. PubMed PMID: 15053410.

707 3. McCall LI, Zhang WW, Matlashewski G. Determinants for the development of
708 visceral leishmaniasis disease. PLoS Pathog. 2013;9(1):e1003053. doi:
709 10.1371/journal.ppat.1003053. PubMed PMID: 23300451; PubMed Central PMCID:
710 PMCPMC3536654.

711 4. Georgiadou SP, Makaritsis KP, Dalekos GN. Leishmaniasis revisited: Current
712 aspects on epidemiology, diagnosis and treatment. J Transl Int Med. 2015;3(2):43-50.
713 doi: 10.1515/jtim-2015-0002. PubMed PMID: 27847886; PubMed Central PMCID:
714 PMCPMC4936444.

715 5. Steverding D. The history of leishmaniasis. Parasit Vectors. 2017;10(1):82. Epub
716 2017/02/17. doi: 10.1186/s13071-017-2028-5. PubMed PMID: 28202044; PubMed
717 Central PMCID: PMCPMC5312593.

718 6. Gonzalez C, Wang O, Strutz SE, Gonzalez-Salazar C, Sanchez-Cordero V, Sarkar
719 S. Climate change and risk of leishmaniasis in North America: predictions from ecological
720 niche models of vector and reservoir species. PLoS Negl Trop Dis. 2010;4(1):e585. Epub
721 2010/01/26. doi: 10.1371/journal.pntd.0000585. PubMed PMID: 20098495; PubMed
722 Central PMCID: PMCPMC2799657.

723 7. McIlwee BE, Weis SE, Hosler GA. Incidence of endemic human cutaneous
724 leishmaniasis in the United States. JAMA Dermatol. 2018;154(9):1032-9. doi:
725 10.1001/jamadermatol.2018.2133. PubMed PMID: 30046836; PubMed Central PMCID:
726 PMCPMC6143046.
727 8. Croft SL, Sundar S, Fairlamb AH. Drug resistance in leishmaniasis. Clin Microbiol
728 Rev. 2006;19(1):111-26. Epub 2006/01/19. doi: 10.1128/CMR.19.1.111-126.2006.
729 PubMed PMID: 16418526; PubMed Central PMCID: PMCPMC1360270.
730 9. Elmahallawy EK, Agil A. Treatment of leishmaniasis: a review and assessment of
731 recent research. Curr Pharm Des. 2015;21(17):2259-75. Epub 2014/12/30. doi:
732 10.2174/1381612821666141231163053. PubMed PMID: 25543123.
733 10. Mann S, Frasca K, Scherrer S, Henao-Martinez AF, Newman S, Ramanan P, et
734 al. A review of leishmaniasis: current knowledge and future directions. Curr Trop Med
735 Rep. 2021;8(2):121-32. Epub 2021/03/23. doi: 10.1007/s40475-021-00232-7. PubMed
736 PMID: 33747716; PubMed Central PMCID: PMCPMC7966913.
737 11. Ponte-Sucre A, Gamarro F, Dujardin JC, Barrett MP, Lopez-Velez R, Garcia-
738 Hernandez R, et al. Drug resistance and treatment failure in leishmaniasis: A 21st century
739 challenge. PLoS Negl Trop Dis. 2017;11(12):e0006052. Epub 2017/12/15. doi:
740 10.1371/journal.pntd.0006052. PubMed PMID: 29240765; PubMed Central PMCID:
741 PMCPMC5730103.
742 12. Handman E, Bullen DV. Interaction of *Leishmania* with the host macrophage.
743 Trends Parasitol. 2002;18(8):332-4. doi: 10.1016/s1471-4922(02)02352-8. PubMed
744 PMID: 12377273.

745 13. Alexander J, Russell DG. The interaction of Leishmania species with
746 macrophages. Adv Parasitol. 1992;31:175-254. Epub 1992/01/01. doi: 10.1016/s0065-
747 308x(08)60022-6. PubMed PMID: 1496927.
748 14. Kima PE. The amastigote forms of Leishmania are experts at exploiting host cell
749 processes to establish infection and persist. Int J Parasitol. 2007;37(10):1087-96. doi:
750 10.1016/j.ijpara.2007.04.007. PubMed PMID: 17543969; PubMed Central PMCID:
751 PMCPMC2043126.
752 15. Ueno N, Wilson ME. Receptor-mediated phagocytosis of Leishmania: implications
753 for intracellular survival. Trends Parasitol. 2012;28(8):335-44. doi:
754 10.1016/j.pt.2012.05.002. PubMed PMID: 22726697; PubMed Central PMCID:
755 PMCPMC3399048.
756 16. Wetzel DM, Rhodes EL, Li S, McMahon-Pratt D, Koleske AJ. The Src kinases Hck,
757 Fgr and Lyn activate Arg to facilitate IgG-mediated phagocytosis and Leishmania
758 infection. J Cell Sci. 2016;129(16):3130-43. Epub 2016/07/01. doi: 10.1242/jcs.185595.
759 PubMed PMID: 27358479; PubMed Central PMCID: PMCPMC5004897.
760 17. Wetzel DM, McMahon-Pratt D, Koleske AJ. The Abl and Arg kinases mediate
761 distinct modes of phagocytosis and are required for maximal *Leishmania* infection. Mol
762 Cell Biol. 2012;32(15):3176-86. Epub 2012/06/06. doi: 10.1128/MCB.00086-12. PubMed
763 PMID: 22665498; PubMed Central PMCID: PMCPMC3434515.
764 18. Ullah I, Barrie U, Kernen RM, Mamula ET, Khuong FTH, Booshehri LM, et al. Src-
765 and Abl-family kinases activate spleen tyrosine kinase to maximize phagocytosis and
766 *Leishmania* infection. J Cell Sci. 2023;136(14). Epub 2023/06/26. doi:

767 10.1242/jcs.260809. PubMed PMID: 37357611; PubMed Central PMCID:
768 PMCPMC10399977.
769 19. Greuber EK, Pendergast AM. Abl family kinases regulate FcgammaR-mediated
770 phagocytosis in murine macrophages. J Immunol. 2012;189(11):5382-92. Epub
771 2012/10/27. doi: 10.4049/jimmunol.1200974. PubMed PMID: 23100514; PubMed Central
772 PMCID: PMCPMC3504141.
773 20. Ortiz MA, Mikhailova T, Li X, Porter BA, Bah A, Kotula L. Src family kinases,
774 adaptor proteins and the actin cytoskeleton in epithelial-to-mesenchymal transition. Cell
775 Commun Signal. 2021;19(1):67. Epub 2021/07/02. doi: 10.1186/s12964-021-00750-x.
776 PubMed PMID: 34193161; PubMed Central PMCID: PMCPMC8247114.
777 21. Cortez D, Reuther G, Pendergast AM. The Bcr-Abl tyrosine kinase activates
778 mitogenic signaling pathways and stimulates G1-to-S phase transition in hematopoietic
779 cells. Oncogene. 1997;15(19):2333-42. Epub 1997/12/11. doi: 10.1038/sj.onc.1201400.
780 PubMed PMID: 9393877.
781 22. Jin A, Kurosu T, Tsuji K, Mizuchi D, Arai A, Fujita H, et al. BCR/ABL and IL-3
782 activate Rap1 to stimulate the B-Raf/MEK/Erk and Akt signaling pathways and to regulate
783 proliferation, apoptosis, and adhesion. Oncogene. 2006;25(31):4332-40. Epub
784 2006/03/07. doi: 10.1038/sj.onc.1209459. PubMed PMID: 16518411.
785 23. Yang S, Liu G. Targeting the Ras/Raf/MEK/ERK pathway in hepatocellular
786 carcinoma. Oncol Lett. 2017;13(3):1041-7. Epub 2017/04/30. doi: 10.3892/ol.2017.5557.
787 PubMed PMID: 28454211; PubMed Central PMCID: PMCPMC5403244.
788 24. Guo YJ, Pan WW, Liu SB, Shen ZF, Xu Y, Hu LL. ERK/MAPK signalling pathway
789 and tumorigenesis. Exp Ther Med. 2020;19(3):1997-2007. Epub 2020/02/28. doi:

790 10.3892/etm.2020.8454. PubMed PMID: 32104259; PubMed Central PMCID:
791 PMCPMC7027163.
792 25. Eblen ST. Extracellular-Regulated Kinases: signaling from Ras to ERK substrates
793 to control biological outcomes. Adv Cancer Res. 2018;138:99-142. Epub 2018/03/20. doi:
794 10.1016/bs.acr.2018.02.004. PubMed PMID: 29551131; PubMed Central PMCID:
795 PMCPMC6007982.
796 26. Verin AD, Liu F, Bogatcheva N, Borbiev T, Hershenson MB, Wang P, et al. Role
797 of ras-dependent ERK activation in phorbol ester-induced endothelial cell barrier
798 dysfunction. Am J Physiol Lung Cell Mol Physiol. 2000;279(2):L360-70. Epub 2000/08/05.
799 doi: 10.1152/ajplung.2000.279.2.L360. PubMed PMID: 10926560.
800 27. Wu X, Dayanand KK, Thylur RP, Norbury CC, Gowda DC. Small molecule-based
801 inhibition of MEK1/2 proteins dampens inflammatory responses to malaria, reduces
802 parasite load, and mitigates pathogenic outcomes. J Biol Chem. 2017;292(33):13615-34.
803 Epub 2017/07/07. doi: 10.1074/jbc.M116.770313. PubMed PMID: 28679535; PubMed
804 Central PMCID: PMCPMC5566520.
805 28. Martinez PA, Petersen CA. Chronic infection by *Leishmania amazonensis*
806 mediated through MAPK ERK mechanisms. Immunol Res. 2014;59(1-3):153-65. Epub
807 2014/05/20. doi: 10.1007/s12026-014-8535-y. PubMed PMID: 24838145; PubMed
808 Central PMCID: PMCPMC4686340.
809 29. Shadab M, Ali N. Evasion of host defence by *Leishmania donovani*: subversion of
810 signaling pathways. Mol Biol Int. 2011;2011:343961. Epub 2011/11/18. doi:
811 10.4061/2011/343961. PubMed PMID: 22091401; PubMed Central PMCID:
812 PMCPMC3199940.

813 30. Olivier M, Gregory DJ, Forget G. Subversion mechanisms by which Leishmania
814 parasites can escape the host immune response: a signaling point of view. Clin Microbiol
815 Rev. 2005;18(2):293-305. Epub 2005/04/16. doi: 10.1128/CMR.18.2.293-305.2005.
816 PubMed PMID: 15831826; PubMed Central PMCID: PMCPMC1082797.
817 31. Ghalib HW, Whittle JA, Kubin M, Hashim FA, el-Hassan AM, Grabstein KH, et al.
818 IL-12 enhances Th1-type responses in human *Leishmania donovani* infections. J
819 Immunol. 1995;154(9):4623-9. Epub 1995/05/01. PubMed PMID: 7722314.
820 32. Bhardwaj S, Srivastava N, Sudan R, Saha B. Leishmania interferes with host cell
821 signaling to devise a survival strategy. J Biomed Biotechnol. 2010;2010:109189. Epub
822 2010/04/17. doi: 10.1155/2010/109189. PubMed PMID: 20396387; PubMed Central
823 PMCID: PMCPMC2852600.
824 33. Yang Z, Mosser DM, Zhang X. Activation of the MAPK, ERK, following *Leishmania*
825 *amazonensis* infection of macrophages. J Immunol. 2007;178(2):1077-85. doi:
826 10.4049/jimmunol.178.2.1077. PubMed PMID: 17202371; PubMed Central PMCID:
827 PMCPMC2643020.
828 34. Mukbel RM, Patten C, Jr., Gibson K, Ghosh M, Petersen C, Jones DE.
829 Macrophage killing of *Leishmania amazonensis* amastigotes requires both nitric oxide
830 and superoxide. Am J Trop Med Hyg. 2007;76(4):669-75. Epub 2007/04/12. PubMed
831 PMID: 17426168.
832 35. Calegari-Silva TC, Pereira RM, De-Melo LD, Saraiva EM, Soares DC, Bellio M, et
833 al. NF-kappaB-mediated repression of iNOS expression in *Leishmania amazonensis*
834 macrophage infection. Immunol Lett. 2009;127(1):19-26. Epub 2009/08/29. doi:
835 10.1016/j.imlet.2009.08.009. PubMed PMID: 19712696.

836 36. Boggiatto PM, Martinez PA, Pullikuth A, Jones DE, Bellaire B, Catling A, et al.
837 Targeted extracellular signal-regulated kinase activation mediated by *Leishmania*
838 *amazonensis* requires MP1 scaffold. Microbes Infect. 2014;16(4):328-36. doi:
839 10.1016/j.micinf.2013.12.006. PubMed PMID: 24463270; PubMed Central PMCID:
840 PMCPMC4023638.
841 37. Uphoff CC, Drexler HG. Eradication of mycoplasma contaminations. Methods Mol
842 Biol. 2013;946:15-26. Epub 2012/11/28. doi: 10.1007/978-1-62703-128-8_2. PubMed
843 PMID: 23179823.
844 38. Ullah I, Gahalawat S, Booshehri LM, Niederstrasser H, Majumdar S, Leija C, et al.
845 An antiparasitic compound from the Medicines for Malaria Venture Pathogen Box
846 promotes *Leishmania* tubulin polymerization. ACS Infect Dis. 2020;6(8):2057-72. Epub
847 2020/07/21. doi: 10.1021/acsinfecdis.0c00122. PubMed PMID: 32686409.
848 39. Wetzel DM, Hakansson S, Hu K, Roos D, Sibley LD. Actin filament polymerization
849 regulates gliding motility by apicomplexan parasites. Mol Biol Cell. 2003;14(2):396-406.
850 doi: 10.1091/mbc.E02-08-0458. PubMed PMID: 12589042; PubMed Central PMCID:
851 PMC149980.
852 40. Pan AA, McMahon-Pratt D. Monoclonal antibodies specific for the amastigote
853 stage of *Leishmania pifanoi*. I. Characterization of antigens associated with stage- and
854 species-specific determinants. J Immunol. 1988;140(7):2406-14. PubMed PMID:
855 2450920.
856 41. Champsi J, McMahon-Pratt D. Membrane glycoprotein M-2 protects against
857 *Leishmania amazonensis* infection. Infect Immun. 1988;56(12):3272-9. PubMed PMID:
858 3182080; PubMed Central PMCID: PMCPMC259734.

859 42. Soong L, Chang CH, Sun J, Longley BJ, Jr., Ruddle NH, Flavell RA, et al. Role of
860 CD4+ T cells in pathogenesis associated with *Leishmania amazonensis* infection. J
861 Immunol. 1997;158(11):5374-83. PubMed PMID: 9164958.
862 43. Soong L, Henard CA, Melby PC. Immunopathogenesis of non-healing American
863 cutaneous leishmaniasis and progressive visceral leishmaniasis. Semin Immunopathol.
864 2012;34(6):735-51. Epub 2012/10/12. doi: 10.1007/s00281-012-0350-8. PubMed PMID:
865 23053396; PubMed Central PMCID: PMCPMC4111229.
866 44. Navas A, Vargas DA, Freudzon M, McMahon-Pratt D, Saravia NG, Gomez MA.
867 Chronicity of dermal leishmaniasis caused by *Leishmania panamensis* is associated with
868 parasite-mediated induction of chemokine gene expression. Infect Immun.
869 2014;82(7):2872-80. doi: 10.1128/IAI.01133-13. PubMed PMID: 24752514; PubMed
870 Central PMCID: PMCPMC4097649.
871 45. Gonzalez-Fajardo L, Fernandez OL, McMahon-Pratt D, Saravia NG. *Ex vivo* host
872 and parasite response to antileishmanial drugs and immunomodulators. PLoS Negl Trop
873 Dis. 2015;9(5):e0003820. Epub 2015/05/30. doi: 10.1371/journal.pntd.0003820. PubMed
874 PMID: 26024228; PubMed Central PMCID: PMC4449175.
875 46. Falchook GS, Lewis KD, Infante JR, Gordon MS, Vogelzang NJ, DeMarini DJ, et
876 al. Activity of the oral MEK inhibitor trametinib in patients with advanced melanoma: a
877 phase 1 dose-escalation trial. Lancet Oncol. 2012;13(8):782-9. Epub 2012/07/19. doi:
878 10.1016/S1470-2045(12)70269-3. PubMed PMID: 22805292; PubMed Central PMCID:
879 PMCPMC4109286.

880 47. Cheng Y, Tian H. Current development status of MEK inhibitors. Molecules.
881 2017;22(10). Epub 2017/09/29. doi: 10.3390/molecules22101551. PubMed PMID:
882 28954413; PubMed Central PMCID: PMCPMC6151813.
883 48. Wong DJ, Robert L, Atefi MS, Lassen A, Avarappatt G, Cerniglia M, et al. Antitumor
884 activity of the ERK inhibitor SCH772984 [corrected] against BRAF mutant, NRAS mutant
885 and wild-type melanoma. Mol Cancer. 2014;13:194. Epub 2014/08/22. doi:
886 10.1186/1476-4598-13-194. PubMed PMID: 25142146; PubMed Central PMCID:
887 PMCPMC4155088.
888 49. Ciuffreda L, Del Bufalo D, Desideri M, Di Sanza C, Stoppacciaro A, Ricciardi MR,
889 et al. Growth-inhibitory and antiangiogenic activity of the MEK inhibitor PD0325901 in
890 malignant melanoma with or without BRAF mutations. Neoplasia. 2009;11(8):720-31.
891 Epub 2009/08/04. doi: 10.1593/neo.09398. PubMed PMID: 19649202; PubMed Central
892 PMCID: PMCPMC2713590.
893 50. Sun Y, Liu WZ, Liu T, Feng X, Yang N, Zhou HF. Signaling pathway of MAPK/ERK
894 in cell proliferation, differentiation, migration, senescence and apoptosis. J Recept Signal
895 Transduct Res. 2015;35(6):600-4. Epub 2015/06/23. doi:
896 10.3109/10799893.2015.1030412. PubMed PMID: 26096166.
897 51. Crowley MT, Costello PS, Fitzer-Attas CJ, Turner M, Meng F, Lowell C, et al. A
898 critical role for Syk in signal transduction and phagocytosis mediated by Fcgamma
899 receptors on macrophages. J Exp Med. 1997;186(7):1027-39. Epub 1997/10/07. doi:
900 10.1084/jem.186.7.1027. PubMed PMID: 9314552; PubMed Central PMCID:
901 PMCPMC2199061.

902 52. Kiefer F, Brumell J, Al-Alawi N, Latour S, Cheng A, Veillette A, et al. The Syk
903 protein tyrosine kinase is essential for Fcgamma receptor signaling in macrophages and
904 neutrophils. Mol Cell Biol. 1998;18(7):4209-20. Epub 1998/06/25. doi:
905 10.1128/MCB.18.7.4209. PubMed PMID: 9632805; PubMed Central PMCID:
906 PMCPMC109005.
907 53. Liu L, Mayes PA, Eastman S, Shi H, Yadavilli S, Zhang T, et al. The BRAF and
908 MEK inhibitors dabrafenib and trametinib: effects on immune function and in combination
909 with immunomodulatory antibodies Targeting PD-1, PD-L1, and CTLA-4. Clin Cancer
910 Res. 2015;21(7):1639-51. Epub 2015/01/16. doi: 10.1158/1078-0432.CCR-14-2339.
911 PubMed PMID: 25589619.
912 54. Shi-Lin D, Yuan X, Zhan S, Luo-Jia T, Chao-Yang T. Trametinib, a novel MEK
913 kinase inhibitor, suppresses lipopolysaccharide-induced tumor necrosis factor (TNF)-
914 alpha production and endotoxin shock. Biochem Biophys Res Commun.
915 2015;458(3):667-73. Epub 2015/02/17. doi: 10.1016/j.bbrc.2015.01.160. PubMed PMID:
916 25684183.
917 55. Boggiatto PM, Jie F, Ghosh M, Gibson-Corley KN, Ramer-Tait AE, Jones DE, et
918 al. Altered dendritic cell phenotype in response to *Leishmania amazonensis* amastigote
919 infection is mediated by MAP kinase, ERK. Am J Pathol. 2009;174(5):1818-26. doi:
920 10.2353/ajpath.2009.080905. PubMed PMID: 19349356; PubMed Central PMCID:
921 PMCPMC2671270.
922 56. Cheeseman KL, Ueyama T, Michaud TM, Kashiwagi K, Wang D, Flax LA, et al.
923 Targeting of protein kinase C-epsilon during Fcgamma receptor-dependent phagocytosis
924 requires the epsilonC1B domain and phospholipase C-gamma1. Mol Biol Cell.

925 2006;17(2):799-813. Epub 2005/12/02. doi: 10.1091/mbc.e04-12-1100. PubMed PMID:
926 16319178; PubMed Central PMCID: PMCPMC1356590.
927 57. Larsen EC, Ueyama T, Brannock PM, Shirai Y, Saito N, Larsson C, et al. A role
928 for PKC-epsilon in Fc gammaR-mediated phagocytosis by RAW 264.7 cells. J Cell Biol.
929 2002;159(6):939-44. Epub 2002/12/25. doi: 10.1083/jcb.200205140. PubMed PMID:
930 12499353; PubMed Central PMCID: PMCPMC2173999.
931 58. Panetti TS, Wilcox SA, Horzempa C, McKeown-Longo PJ. Alpha v beta 5 integrin
932 receptor-mediated endocytosis of vitronectin is protein kinase C-dependent. J Biol Chem.
933 1995;270(31):18593-7. Epub 1995/08/04. doi: 10.1074/jbc.270.31.18593. PubMed
934 PMID: 7543105.
935 59. Roy N, Chakraborty S, Paul Chowdhury B, Banerjee S, Halder K, Majumder S, et
936 al. Regulation of PKC mediated signaling by calcium during visceral leishmaniasis. PLoS
937 One. 2014;9(10):e110843. Epub 2014/10/21. doi: 10.1371/journal.pone.0110843.
938 PubMed PMID: 25329062; PubMed Central PMCID: PMCPMC4201563.
939 60. Zheleznyak A, Brown EJ. Immunoglobulin-mediated phagocytosis by human
940 monocytes requires protein kinase C activation. Evidence for protein kinase C
941 translocation to phagosomes. J Biol Chem. 1992;267(17):12042-8. Epub 1992/06/15.
942 PubMed PMID: 1376316.
943 61. Arthur JS, Ley SC. Mitogen-activated protein kinases in innate immunity. Nat Rev
944 Immunol. 2013;13(9):679-92. Epub 2013/08/21. doi: 10.1038/nri3495. PubMed PMID:
945 23954936.
946 62. Buxbaum LU, Scott P. Interleukin 10- and Fcgamma receptor-deficient mice
947 resolve *Leishmania mexicana* lesions. Infect Immun. 2005;73(4):2101-8. Epub

948 2005/03/24. doi: 10.1128/IAI.73.4.2101-2108.2005. PubMed PMID: 15784551; PubMed
949 Central PMCID: PMCPMC1087424.
950 63. Tada S, Anazawa T, Shindo T, Yamane K, Inoguchi K, Fujimoto N, et al. The MEK
951 inhibitor trametinib suppresses Major Histocompatibility Antigen-mismatched rejection
952 following pancreatic islet transplantation. Transplant Direct. 2020;6(9):e591. Epub
953 2020/08/28. doi: 10.1097/TXD.0000000000001045. PubMed PMID: 32851124; PubMed
954 Central PMCID: PMCPMC7423917.
955

956 **8. LIST OF FIGURES**

957 **Figure 1.** The MAPK/ERK pathway is required for optimal amastigote uptake.

958 **Figure 2**. MAPK/ERK are activated during *Leishmania* uptake by Mϕ.

959 **Figure 3.** PMA activates ERK1/2 to modulate amastigote uptake.

960 **Figure 4.** SYK and Arg/Abl stimulate ERK1/2 phosphorylation during amastigote
961 uptake.

962 **Figure 5.** ERK 1/2's role in *Leishmania* uptake is greater than for phagocytosis of
963 beads.

964 **Figure 6.** MAPK/ERK permit efficient infection in a mouse model of cutaneous
965 leishmaniasis.

966 **Table 1.** Ongoing trametinib treatment during *L. amazonensis* infection has
967 limited effects on Th1 vs Th2 responses.

968 **Table 2.** Cytokine and chemokine profiles in diluent versus trametinib-treated,
969 *Leishmania*-infected mice.

970

971 **9. LIST OF SUPPLEMENTARY MATERIALS**

972 **Supplemental Figure 1.** MAPK/ERK inhibitors decrease uptake and survival of
973 *L. amazonensis* promastigotes and amastigotes.

974 **Supplemental Figure 2.** Inhibiting kinases upstream of ERK during *L.*
975 *amazonensis* uptake decreases ERK phosphorylation.

976 **Supplemental Figure 3.** Inhibiting ERK1/2 has minimal effects on the uptake of
977 opsonized beads.

978 **Supplemental Figure 4.** Actin-based phagocytic cups are brighter in trametinib-
979 treated Mϕs taking up *Leishmania* amastigotes compared to DMSO-treated Mϕs.

980 **Supplemental Table 1.** Trametinib initiated during *L. amazonensis* infection has
981 limited effects on Th1 vs Th2 responses.

982 **Supplemental Table 2.** Cytokine and chemokine profiles from *Leishmania*-
983 infected mice treated once lesions are visible.

984 **Supplemental Table 3.** Antibodies.

985 **10. FIGURES AND LEGENDS**

986 **Figure 1**

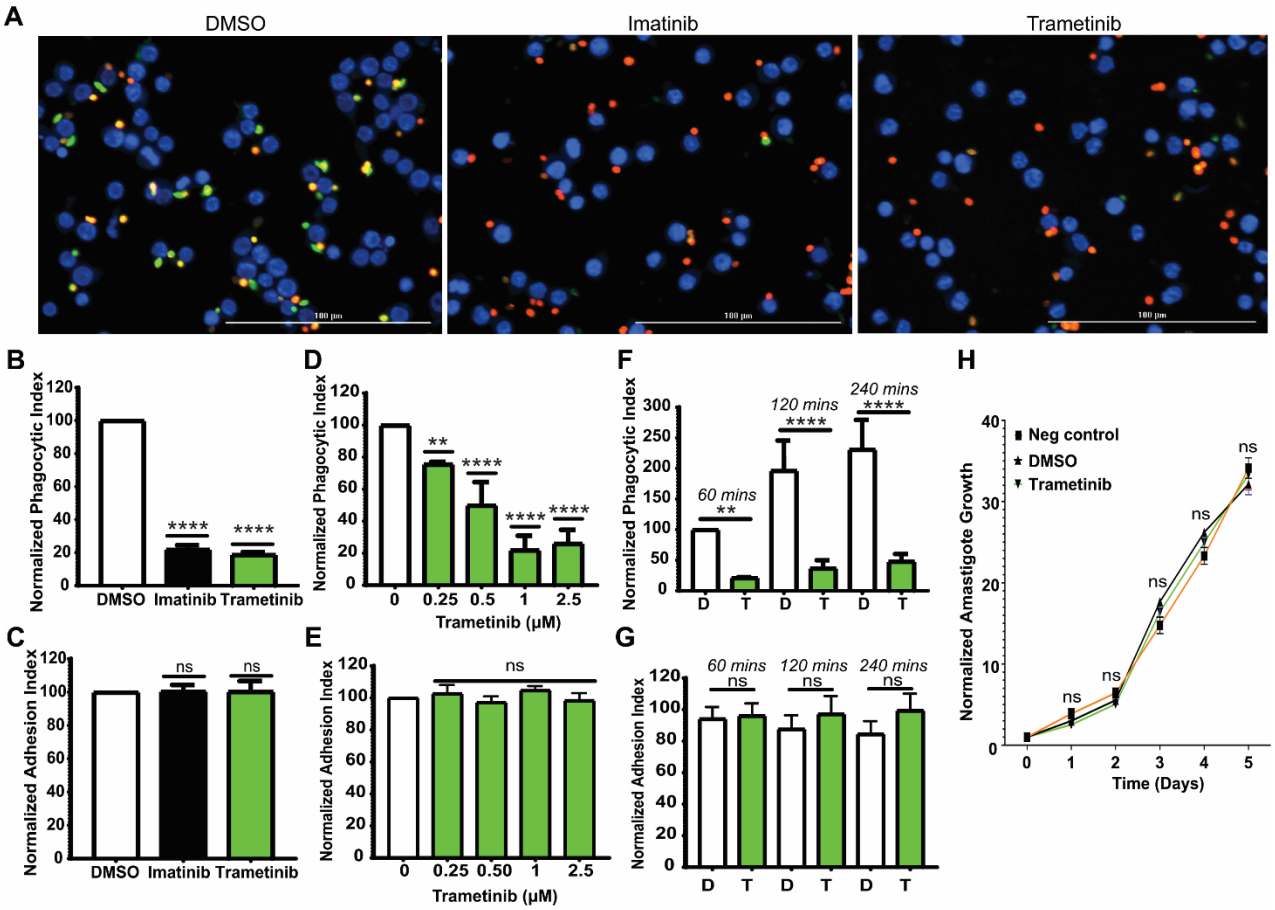

987

988 **Figure 1. The MAPK/ERK pathway is required for optimal amastigote**

989 **uptake. (A)** Trametinib decreases IgG-opsonized amastigote uptake. RAW 264.7

990 cells were treated with 3.3 μM imatinib, 1 μM trametinib or DMSO for 2 h, and 10

991 IgG-opsonized amastigotes were incubated per RAW 264.7 cell for 2 h at 37°C.

992 An immunofluorescence assay distinguished between intracellular (green) and

993 extracellular (red + green) amastigotes. Nuclei are labeled with Hoescht 33342

994 (blue). Scale bar, 100 μm. **(B)** Graph showing the mean phagocytic index (PI) ±

995 standard deviation (SD) for RAW 264.7 cells normalized to DMSO for each

996 experiment (100%), quantified from n = 6 biological experiments. Comparisons

997 between imatinib and trametinib by ANOVA were nonsignificant. **(C)** Imatinib and
998 trametinib do not affect the total (external + internal) number of amastigotes per
999 100 RAW cells (termed an adhesion index). Shown are percentages of total
1000 amastigotes per 100 imatinib-treated and trametinib-treated RAW 264.7 cells
1001 relative to DMSO-treated cells for the experiment shown in B. **(D)** Titration of
1002 trametinib demonstrates that the reduction of amastigote internalization is
1003 maximal at ~100x the purified MEK1/2 IC_{50}. RAW 264.7 cells were treated with
1004 increasing doses of trametinib (0.25, 0.5, 1, or 2.5 μM) or DMSO. Bar graph
1005 shows the mean PI ± SD for trametinib-treated samples relative to DMSO-treated
1006 samples for each experiment (100%) for 4 biological experiments. **(E)** The
1007 adhesion index for amastigotes from experiment in D is not affected by
1008 increasing doses of trametinib. Experiment performed as in C. **(F)** The relative
1009 decrease in PI for trametinib-treated samples persists even after prolonged
1010 incubation. RAW 264.7 cells were treated with DMSO (D) or 1 μM trametinib (T)
1011 prior to addition of IgG-opsonized amastigotes for 1 h, 2 h, or 4 h, as indicated.
1012 Shown is the mean PI ± SD for each time point for the trametinib-treated
1013 condition, relative to the DMSO-treated condition, calculated from 4 biological
1014 experiments. **(G)** Treating samples with trametinib for prolonged periods does not
1015 affect the adhesion index for amastigotes. Shown are the total number of
1016 amastigotes (internal + external) per 100 RAW 264.7 cells for the experiments
1017 performed in F. For all experiments, ** $P < 0.01$, **** $P < 0.0001$, ns =
1018 nonsignificant compared to the relevant DMSO-treated category by ANOVA. **(H)**
1019 Trametinib is not toxic to amastigotes. Shown is one representative experiment

1020 of five experiments with two technical replicates following the number of
1021 amastigotes growing in untreated, DMSO-treated, or trametinib-treated media
1022 over 5 days relative to on day 0. ns, $P > 0.05$ compared to DMSO category by
1023 ANOVA.
1024

1025 **Figure 2**

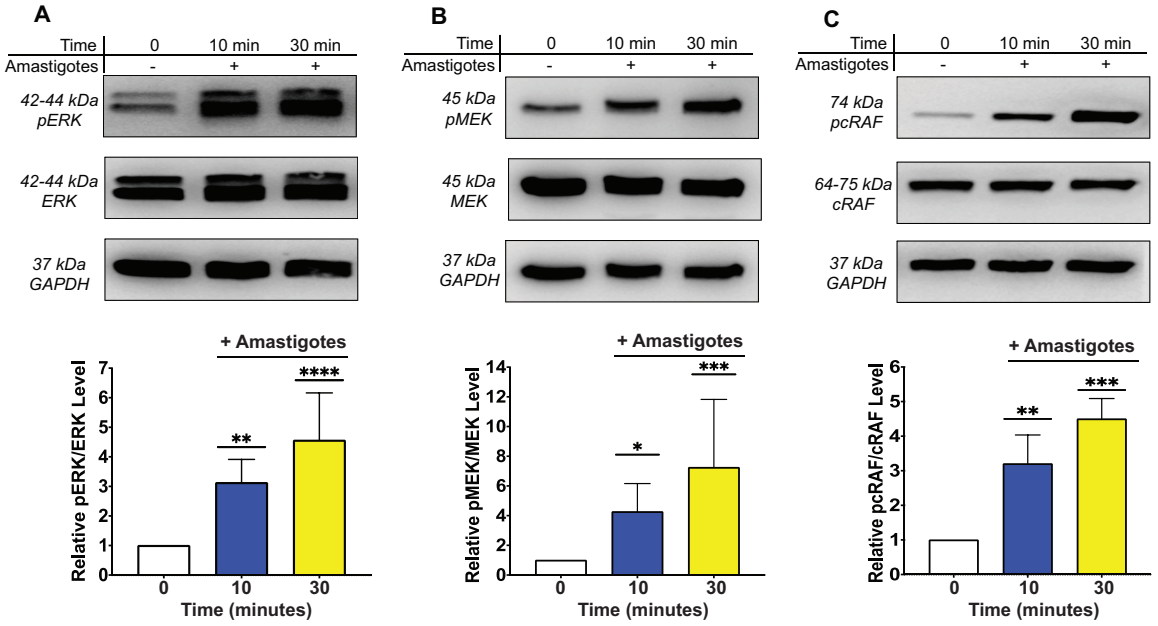

1026

1027 **Figure 2**. **MAPK/ERK are activated during *Leishmania* uptake by Mϕ.**

1028 Amastigotes were added to ≥ 70% confluent RAW 264.7 cells. Equal amounts of

1029 protein from whole lysates were employed for each category. **Top:**

1030 Representative blots displaying relative activation of MAPK/ERK. Phosphorylated

1031 **(A)** ERK1/2, **(B)** MEK1/2, **(C)** cRaf (Raf-1) and the corresponding total proteins

1032 were detected by Western Blot. An unrelated protein, GAPDH, is shown as an

1033 additional loading control. **Bottom:** Quantification of phosphorylated MAPK/ERK

1034 levels. Graphs shown in **(A)** for ERK1/2, **(B)** for MEK1/2, and **(C)** for cRaf

1035 represent mean ± SD of relative phosphorylated kinase levels, normalized to total

1036 kinase levels, for at least 3 biological replicates per condition. * $P < 0.05$, ** $P <$

1037 0.01, *** $P < 0.001$, **** $P < 0.0001$ by ANOVA compared to the 0 m time point

1038 for each set of kinases.

1039

1040 **Figure 3**

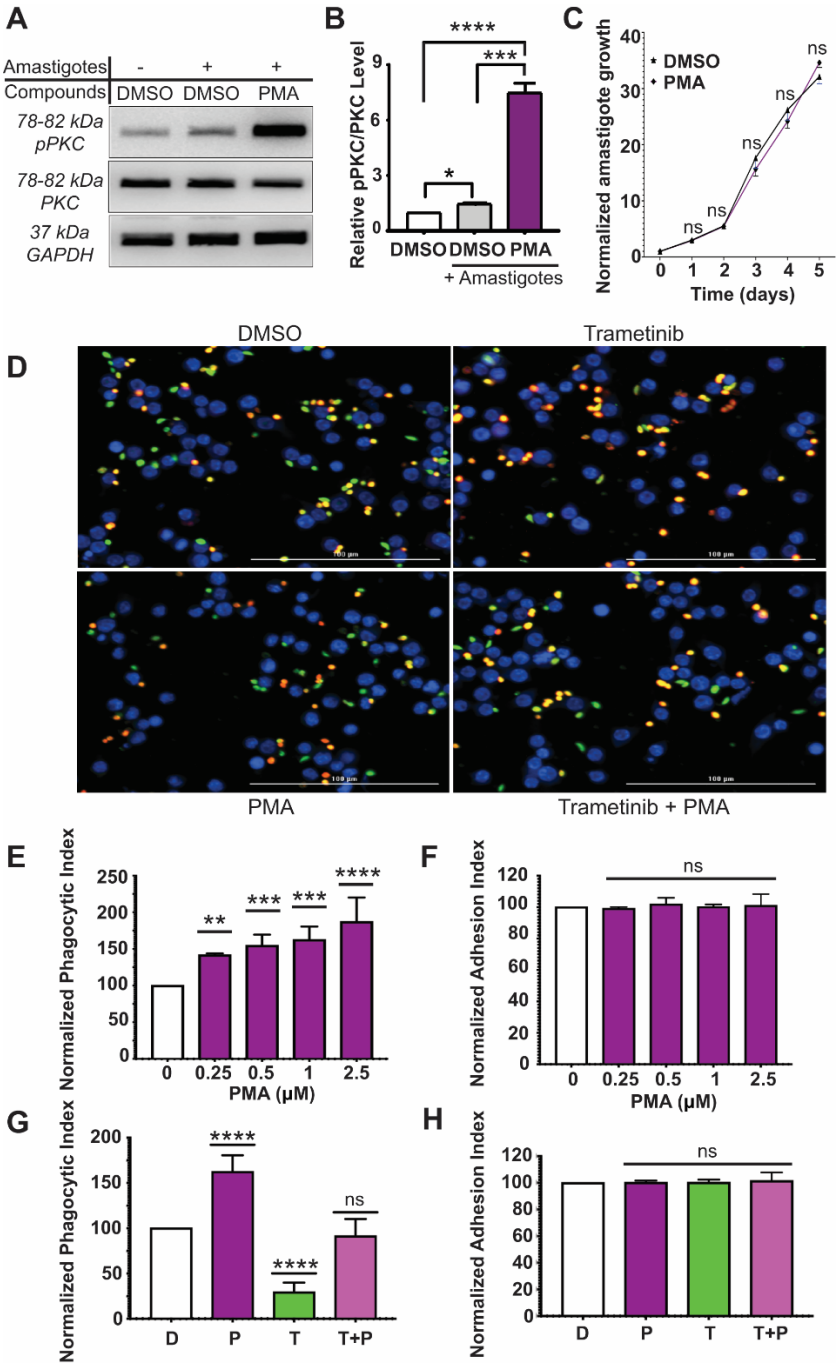

1041

1042 **Figure 3. PMA activates ERK1/2 to modulate amastigote uptake**. **(A, B)** PKC

1043 typically is only slightly activated during amastigote uptake. PMA serves as a

1044 positive control. Amastigotes were added to monolayers of RAW 264.7 cells and

1045 processed as above. Shown are **(A)** representative blots demonstrating and **(B)**

1046 bar graphs quantifying relative activation of pPKC/PKC. * $P < 0.05$, *** $P < 0.001$,
1047 **** $P < 0.0001$ compared with samples indicated by brackets (ANOVA). n = 3
1048 experiments. **(C)** PMA is not toxic to amastigotes. Shown is one representative
1049 experiment of five experiments with two technical repeats following the number of
1050 amastigotes growing in DMSO-treated or PMA-treated media over 5 days relative
1051 to on day 0. ns, $P > 0.05$ compared to DMSO category by ANOVA. **(D)**
1052 Representative image demonstrating that PMA rescues trametinib inhibition of
1053 *Leishmania* amastigote uptake. BMDM were treated with DMSO, 1 μM PMA, 1
1054 μM trametinib or a combination of 1 μM trametinib and 1 μM PMA prior to
1055 incubation with IgG-opsonized amastigotes for 2 hours. **(E)** PMA increases IgG-
1056 opsonized amastigote uptake. BMDM were treated with DMSO or increasing
1057 doses of PMA (0.25, 0.5, 1, 2.5 μM) prior to incubation with IgG-opsonized
1058 amastigotes for the times indicated. n = 4 experiments. ** $P < 0.01$, *** $P < 0.001$,
1059 **** $P < 0.0001$ compared to DMSO category by ANOVA. **(F)** PMA does not
1060 affect the adhesion index for amastigotes. ns, not significant by ANOVA. **(G)**
1061 Mean PI ± SD for BMDM treated with trametinib/PMA relative to DMSO-treated
1062 samples for each experiment (100%), obtained from 3 biological experiments.
1063 **** $P < 0.0001$, ns = nonsignificant by ANOVA compared to DMSO-treated
1064 sample. **(H)** Trametinib/PMA does not affect amastigote adhesion for the
1065 experiment shown in G.
1066

1067 **Figure 4**

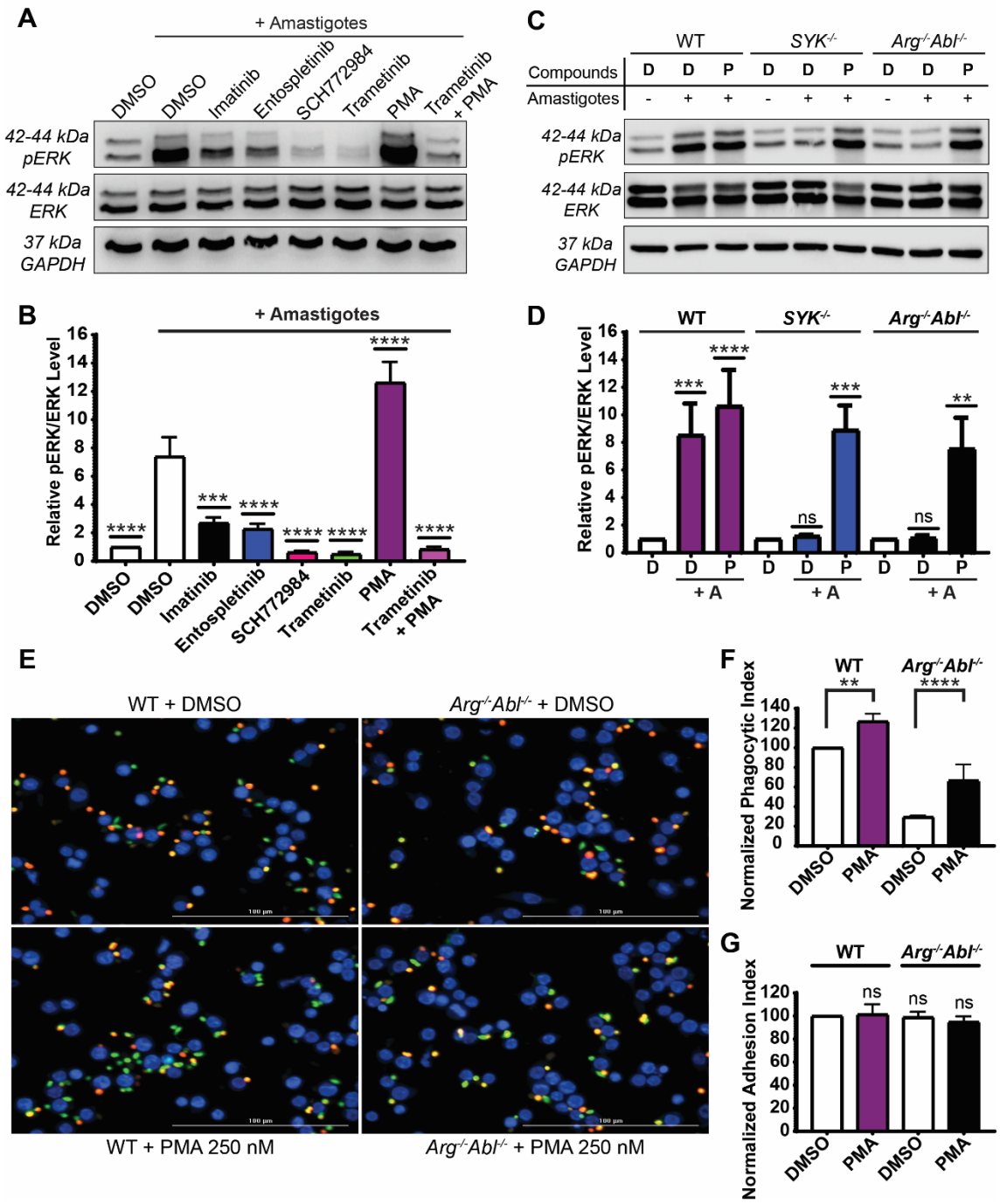

1068

1069 **Figure 4. SYK and Arg/Abl stimulate ERK1/2 phosphorylation during**

1070 **amastigote uptake. (A)** Phosphorylation of ERK1/2 in RAW 264.7 cells is

1071 induced upon amastigote uptake and is decreased by imatinib (Arg/Abl inhibitor),

1072 entospletinib (SYK inhibitor), SCH772984 (ERK1/2 inhibitor), and trametinib
1073 (MEK1/2 inhibitor). PMA serves as a positive control for pERK stimulation. RAW
1074 264.7 cells were allowed to adhere to plates, and then treated with compounds or
1075 DMSO prior to IgG-opsonized amastigote addition, lysis, and immunoblotting.
1076 Representative immunoblots of pERK1/2 (top) and total ERK1/2 (bottom) [with
1077 (+) or without (–) amastigotes] are shown. **(B)** Relative pERK levels, normalized
1078 to ERK1/2 levels, among categories shown in A. Levels of pERK are normalized
1079 to amastigote-exposed DMSO-treated RAW 264.7 cells (100%). 5 biological
1080 replicates are quantified. *** $P < 0.001$, **** $P < 0.0001$ compared with
1081 amastigote-stimulated, DMSO-treated RAW 264.7 cells (ANOVA). **(C)**
1082 Phosphorylation of ERK1/2 induced upon FcγR engagement is decreased
1083 in *SYK*$^{-/-}$ and *Arg*$^{-/-}$*Abl*$^{-/-}$ BMDM compared to WT BMDM. Shown is a
1084 representative immunoblot of pERK1/2 (top) and total ERK1/2 (bottom) in WT,
1085 *SYK*$^{-/-}$ and *Arg*$^{-/-}$*Abl*$^{-/-}$ BMDM treated with DMSO (D) or PMA (P), ± incubation
1086 with amastigotes. **(D)** Graph showing relative levels of pERK1/2, normalized to
1087 ERK1/2 levels, among WT, *SYK*$^{-/-}$, and *Arg*$^{-/-}$*Abl*$^{-/-}$ BMDM treated with DMSO
1088 (D) or PMA (P), ± amastigotes (A). ** $P < 0.01$, *** $P < 0.001$, **** $P < 0.0001$, ns:
1089 not significant by ANOVA (n = 6 experiments), compared to DMSO + amastigote
1090 category for each condition. **(E-G)** Primary cells lacking Arg and Abl exhibit
1091 decreases in amastigote uptake, but PMA can partially rescue this amastigote
1092 internalization defect. **(E)** Representative image performed as in Fig 1. **(F)** Mean
1093 phagocytic index ± SD for PMA-treated and/or *Arg*$^{-/-}$ *Abl*$^{-/-}$ BMDM relative to WT
1094 DMSO-treated BMDM. **(G)** DMSO and PMA do not affect the adhesion indexes

1095 for the experiments shown in F. n for F-G = 3 experiments. ** $P < 0.01$; *** $P <$

1096 0.001; **** $P < 0.0001$; ns, not significant compared with DMSO-treated WT

1097 BMDM (ANOVA).

1098

1099 **Figure 5**

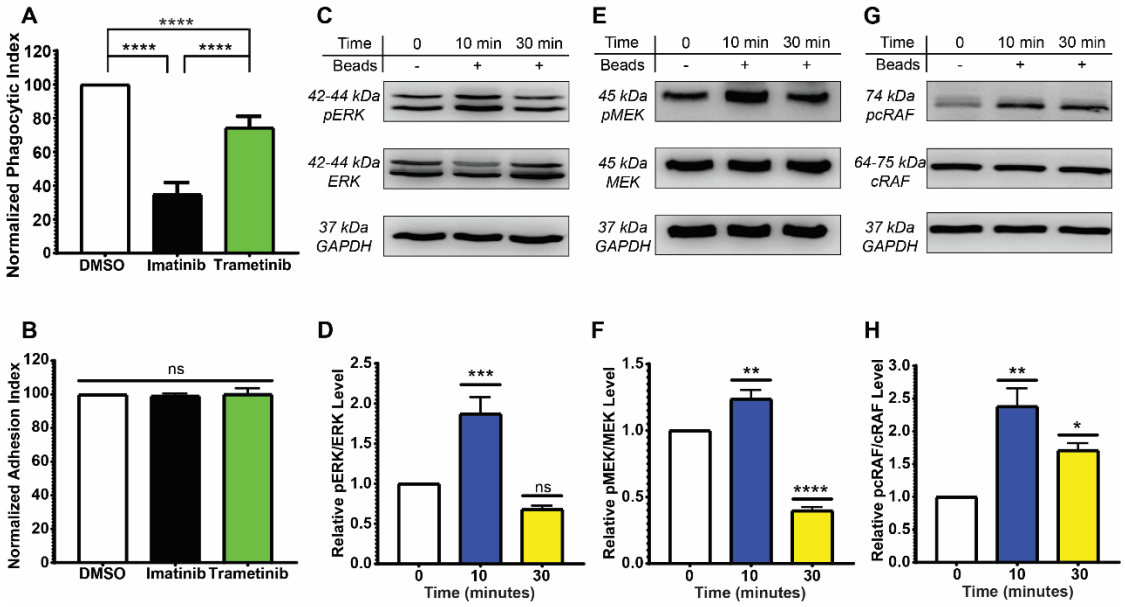

1100

1101 **Figure 5. ERK 1/2's role in *Leishmania* uptake is greater than for**

1102 **phagocytosis of beads**. **(A)** Trametinib mildly decreases bead internalization.

1103 RAW 264.7 cells were treated with 3.3 μM imatinib, 1 μM trametinib or DMSO for

1104 2 hr. prior to addition of 10 IgG-opsonized beads per RAW 264.7 cell for 2 h at

1105 37°C. Treating RAW 264.7 cells with trametinib decreases uptake of IgG-

1106 opsonized beads to a lesser degree than imatinib. Graph shows the mean PI ±

1107 SD for each category, normalized to DMSO (100%). **** $P < 0.0001$, ns: not

1108 significant compared to indicated categories by ANOVA (n = 6 biological

1109 experiments). **(B)** Imatinib and trametinib does not affect the adhesion index for

1110 beads in the experiments shown in A. **(C-H)** IgG-coated beads activate the

1111 MAPK/ERK pathway, but phosphorylation is not sustained. Beads were added to

1112 > 70% confluent RAW 264.7 cells and experiments were processed as in Fig 2.

1113 Top: Phosphorylated forms of **(C)** ERK, **(E)** MEK1/2, **(G)** cRaf and the

1114 corresponding total kinase were detected by Western blotting. Bottom: Relative

1115 activation was quantified for **(D)** ERK, **(F)** MEK1/2, and **(H)** cRaf, using the

1116 methods described in Fig 2. * $P < 0.05$, ** $P < 0.01$, *** $P < 0.001$, **** $P < 0.0001$

1117 and ns: not significant compared to 0 m timepoint by ANOVA ($n \geq 3$

1118 experiments).

1119

1120 **Figure 6**

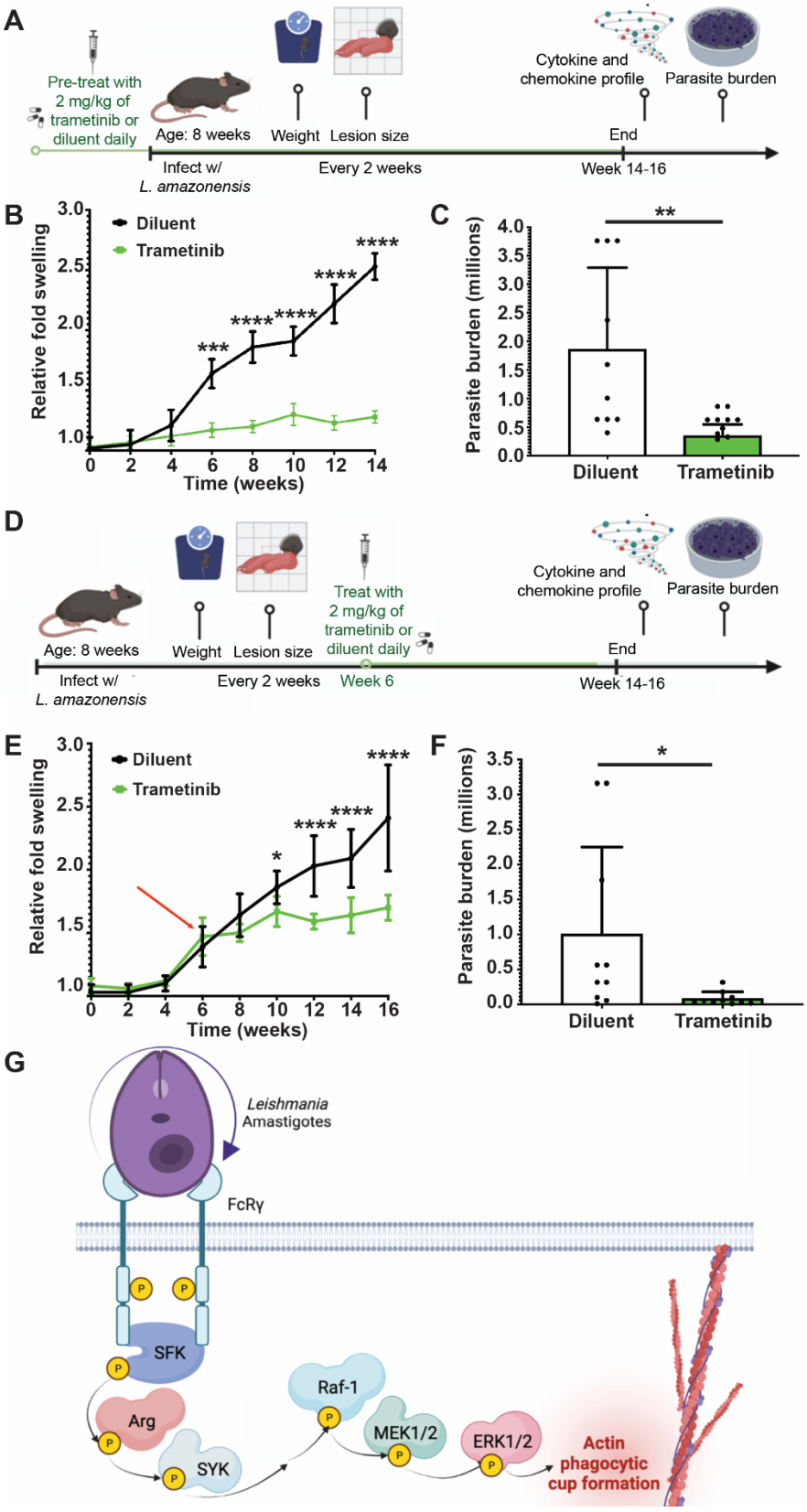

1121

1122 **Figure 6. MAPK/ERK permit efficient infection in a mouse model of**
1123 **cutaneous leishmaniasis. (A)** Mouse footpad model for cutaneous
1124 leishmaniasis. C57BL/6 mice diluent and trametinib-treated groups were injected
1125 with promastigotes in the hind footpad. Mice were given 2 mg/kg body weight of
1126 trametinib or an equal volume of diluent by oral gavage daily, starting 7 days
1127 before infection and continuing until the mice were euthanized. Two experiments
1128 were performed. Shown in the following panels is one representative experiment
1129 containing 10 female mice per group. **(B)** Trametinib given prior to infection
1130 reduces lesion size in mice. Depth of foot swelling was monitored with calipers by
1131 a blinded investigator. Results represent the mean ± SD foot size increase over
1132 the uninfected foot (normalized to 1). The control (diluent) and drug-treated
1133 groups were compared to swelling at time 0 by ANOVA; * $P < 0.05$, **** $P <$
1134 0.0001, ns, not significant. **(C)** Trametinib given prior to infection significantly
1135 reduces parasite burden. Parasite burdens in infected footpads were determined
1136 by limiting dilution as described in *Materials and Methods*. Plotted is the mean
1137 number of parasites (*i.e.*, parasite burden) in millions at the end of the
1138 experiment shown in B ± SD. In this example, there were 1.41×10^6 parasites in
1139 the control mice versus 2.03×10^5 parasites in the trametinib-treated mice. *$P <$
1140 0.05 (two-tailed *t*-test). **(D)** C57BL/6 mice diluent and trametinib-treated groups
1141 were injected with *L. amazonensis* promastigotes as above. Starting 6 weeks
1142 after inoculation (arrow), mice were given 2 mg/kg body weight of trametinib or
1143 vehicle by oral gavage daily and continuing until the experiment was terminated.
1144 **(E)** Trametinib given once lesions have begun reduces lesion size in trametinib-

1145 treated mice compared to diluent-treated mice. Arrow shows start time of drug
1146 treatment. Shown is one representative experiment containing 10 female mice
1147 per group. Statistics calculated as in B. **(F)** Lesions in mice treated with
1148 trametinib 6 weeks after infection contain fewer *Leishmania* parasites than
1149 control mice. Plotted is the mean ± SD lesion parasite burden in millions at the
1150 end of the experiment shown in E; in this example, there were 1.01 x 10^6
1151 parasites in the control mice versus 8.29 x 10^4 parasites in the trametinib-treated
1152 mice (>10-fold reduction). *P <0.05 (two-tailed t-test). (**G**) MAPK/ERK signal
1153 transduction in Mϕ facilitates *Leishmania* uptake and pathogenesis. Upon FcγR
1154 ligation by amastigotes, SFK, Arg, and SYK are activated and relay signals to the
1155 MAPK/ERK pathway, which allows the internalization of *Leishmania*. Diagrams
1156 created with Biorender.
1157

1158 **Table 1**

Experiment	Ratio	DMSO - High	Trametinib - High	DMSO - Low	Trametinib - Low
Trametinib prior to infection	**IFN Gamma/IL-4**	1.86	1.35	1.75	1.05
	IFN Gamma/IL-13	0.78	0.11	0.75	0.09
	IFN Gamma/IL-4+ IL-10+ IL-13	0.55	0.10	0.52	0.08

1159

1160 **Table 1. Ongoing trametinib treatment during *L. amazonensis* infection has**
1161 **limited effects on Th1 vs Th2 responses.** Effects of trametinib during *L.*
1162 *amazonensis* infection on cytokine secretion. Shown are profiles of draining
1163 lymph nodes isolated from diluent (DMSO) versus trametinib-treated mice treated
1164 prior to inoculation as described in methods. High refers to high stimulation with a
1165 lysate of 1 X 10^6 parasites and low refers to low stimulation with 1 X 10^5
1166 parasites. Ratios of IFNγ: IL-4, IFNγ: IL-13, and IFNγ: IL-4+10+13 were
1167 calculated from the data shown in Table 2. Trametinib may skew towards a Th2
1168 response, which should not promote lesion healing.

1169

1170 **Table 2**

Experiment	Cytokine	Treatment	Cytokine secretion (pg) after					
			Con A stimulation		High stimulation		Low treatment	
			AVG	STD	AVG	STD	AVG	STD
Trametinib prior to infection	**IFN Gamma**	DMSO	6.70	6.83	6.06	5.82	5.83	5.16
		Trametinib	0.48	0.64	0.73	1.05	0.58	0.75
		p-value	**0.01**		**0.01**		**0.005**	
	IL-1 BETA	DMSO	0.88	0.51	0.97	0.48	0.73	0.46
		Trametinib	0.45	0.12	0.42	0.11	0.39	0.09
		p-value	**0.02**		**0.002**		**0.03**	
	IL-12/IL23p40	DMSO	5.56	2.97	5.24	2.49	6.04	3.06
		Trametinib	3.28	1.18	3.39	0.79	3.53	1.31
		p-value	**0.04**		**0.04**		**0.03**	
	IL-13	DMSO	5.08	3.04	7.72	2.47	7.78	3.07
		Trametinib	7.01	2.27	6.83	1.10	6.57	1.15
		p-value	NS		NS		NS	
	IL-17A	DMSO	0.48	0.24	0.65	0.14	0.53	0.27
		Trametinib	0.59	0.09	0.74	0.25	0.53	0.25
		p-value	NS		NS		NS	
	IL-4	DMSO	2.36	1.26	3.26	1.89	3.32	2.57
		Trametinib	0.49	0.64	0.54	0.68	0.55	0.70

		p-value	**0.0006**		**0.0004**		**0.004**	
	TNF ALPHA	DMSO	2.98	1.6	2.68	2.10	2.45	1.22
		Trametinib	2.85	2.30	2.23	0.96	1.75	1.45
		p-value	NS		NS		NS	
	IL-10	DMSO	.008	.007	.02	.009	.009	.01
		Trametinib	8.94	8.78	8.36	10.44	5.16	1.06
		p-value	**0.005**		**0.02**		**0.0001**	
	MCP-1	DMSO	25.56	14.87	25.07	12.31	27.90	10.54
		Trametinib	7.23	6.43	7.23	5.87	7.23	6.56
		p-value	**0.002**		**0.0006**		**0.0001**	
	MIP-1 ALPHA	DMSO	4.69	3.95	3.93	2.77	4.62	2.96
		Trametinib	1.36	0.41	1.44	0.86	1.44	0.88
		p-value	**0.02**		**0.01**		**0.004**	

Table 2. Cytokine and chemokine profiles in diluent versus trametinib-treated, *Leishmania*-infected mice. Shown are profiles of draining lymph nodes isolated from DMSO versus trametinib mice treated prior to infection as described in methods. For high stimulation categories, a lysate containing 1 X 10^6 *L. amazonensis* was added, and for low stimulation categories, a lysate containing 1 X 10^5 parasites was added. Post 14-16 weeks, mice were sacrificed and multiplex chemokine ELISAs were performed on harvested lymph node

1179 supernatants. *P* values were determined by two-tailed *t*-tests and are listed if $P <$

1180 0.1. Bold: $P \leq 0.05$.

1181